

This document is confidential and is proprietary to the American Chemical Society and its authors. Do not copy or disclose without written permission. If you have received this item in error, notify the sender and delete all copies.

Selectivity in the photo-Fries rearrangement of some aryl benzoates in green and sustainable media. Preparative and mechanistic studies.

Journal:	<i>The Journal of Organic Chemistry</i>
Manuscript ID	jo-2019-00334a.R2
Manuscript Type:	Article
Date Submitted by the Author:	n/a
Complete List of Authors:	Siano, Gastón; Universidad de Buenos Aires Facultad de Ciencias Exactas y Naturales, Química Orgánica Crespi, Stefano; Università degli Studi di Pavia, Department of Chemistry Mella, Mariella; Università degli Studi di Pavia, of Chemistry Bonesi, Sergio; University of Buenos Aires, Organic Chemistry

SCHOLARONE™
Manuscripts

1
2 **Selectivity in the photo-Fries rearrangement of some aryl benzoates in green and sustainable**
3
4 **media. Preparative and mechanistic studies.**
5
6
7

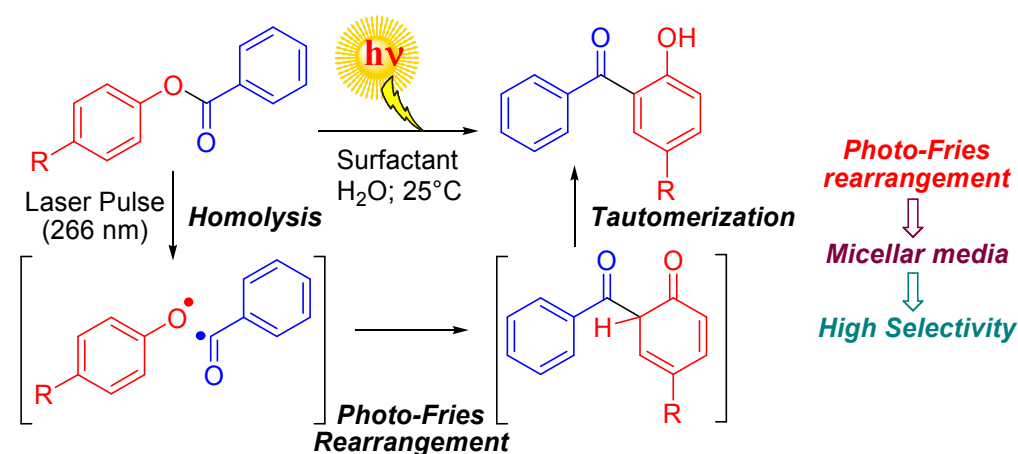
8 **Gastón Siano^a, Stefano Crespi^b, Mariella Mella^b and Sergio M. Bonesi^{*,a,b}**
9
10

11
12
13 ^a *Departamento de Química Orgánica, CIHIDECAR – CONICET, 3^{er} Piso, Pabellón 2, Ciudad*
14 *Universitaria, Facultad de Ciencias Exactas y Naturales, University of Buenos Aires, Buenos Aires,*
15 *1428, Argentina. Phone: +541145763346.*
16
17
18

19
20 ^b *Dipartimento di Chimica, Sezione Chimica Organica, v.le Taramelli 12, 27100, University of Pavia,*
21 *Pavia, Italy.*
22
23

24
25 E-mail: smbonesi@qo.fcen.uba.ar
26
27
28

29 **Table of content.**
30
31



49 **Abstract.** Irradiation of a series of p-substituted aryl benzoates under N₂ atmosphere in homogeneous
50 and micellar media was investigated by means of steady-state condition and of time-resolved
51 spectroscopy. A notable selectivity in favor of the 2-hydroxybenzophenone derivatives was observed in
52 micellar media. The benzophenone derivatives were the main photoproduct. On the other hand, in
53
54
55
56
57
58
59
60

1
2 homogeneous media (cyclohexane, acetonitrile, and methanol) the observed product distribution was
3
4 entirely different, viz. substituted 2-hydroxybenzophenones, *p*-substituted phenols, benzyl and benzoic
5
6 acid were found. The binding constants in the surfactant were also measured and NOESY experiments
7
8 showed that the aryl benzoates were located in the hydrophobic core of the micelle. Laser flash
9
10 photolysis experiments led to the characterization of both *p*-substituted phenoxy radical and substituted
11
12 2-benzoylcyclohexadienone transients in homogeneous and micellar environment.
13
14
15
16
17

18 **Introduction.**

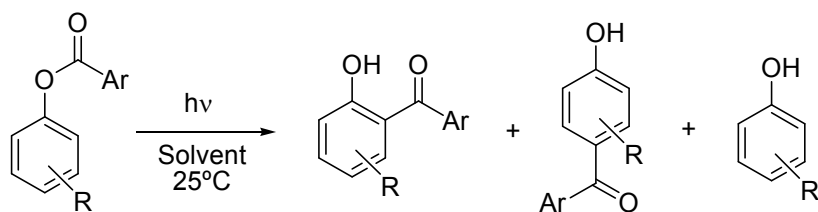
19
20 Photochemical reactions grant access to a variety of scaffolds difficult, if not impossible, to access
21
22 through thermal chemistry. However, the energetic advantage of populating the excited states is often
23
24 paid with a lack of selectivity in product formation. For this reason, reactions involving intermediates
25
26 such as radical pairs or radical-ion pairs represent a significant challenge regarding product distribution
27
28 for the synthetic organic photochemist. Zeolites, micelles, polyolefin films, cavitands, dendrimers, etc.,
29
30 as a useful heterogeneous media, can be helpful to direct the selectivity of photoproducts in
31
32 photoinduced reactions.¹
33
34
35

36 Surfactants are amphiphilic molecules and aggregation in solution to form micelles can be
37
38 achieved when their concentration is 100 times higher than the critical micellar concentration (*cmc*).
39
40 Then, micelles solubilize efficiently hydrophobic compounds in water, albeit micelles are not static
41
42 species showing a dynamic equilibrium.² Also, micelle can concentrate guest molecules into relatively
43
44 small effective volumes promoting their re-encounter consequently.^{1c} Inside the homophobic core of
45
46 the micelles, significant cage effects are observed when compared to homogeneous media, with
47
48 magnitudes impossible to explain considering the sole microviscosity in the constrained environment.
49
50 The main reason for this behavior is based on the hydrophobicity of the solutes where inhibition of
51
52 their diffusion into the aqueous phase is noteworthy. Thus, the reaction intermediates show a high
53
54 lifetime in the restricted hydrophobic core of the micelle. For example, geminate radical pairs that are
55
56
57
58
59
60

1 produced photochemically within the micellar core, have their rotational and translational mobility
2 constrained inside the micelles.² Indeed, the mobility restricted within the hydrophobic cores of
3 radicals, radical cations, or other reactive intermediates limits unwanted reactions (*e.g.* radical–radical
4 self-quenching reactions) and the access of adventitious reagents (*e.g.* water and oxygen) that would
5 cause their collapse in solution. Therefore, micellar solution can induce a product distribution and a
6 relative chemical yield that can be significantly different when compared with homogeneous
7 conditions.^{1,2}

18 There has been many studies on the control of the reactivity of radical species generated within
19 the hydrophobic core of the micelle and some physical parameters (*e.g.* electrostatic, polarity,
20 hydrophobic interactions, viscosity, as well as hydrogen-bonding solvation) may be involved in
21 determining their reactivities.³ Also, several studies directed to analyze and quantify the reactivity,
22 selectivity, and efficiency of micellar cage on photochemical reactions in water have been carried out.
23

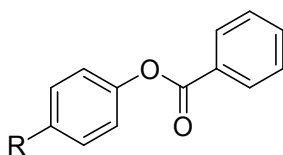
29 Among the vast number of photochemical transformations, a particular example is represented
30 by the photo-Fries rearrangement. Anderson and Reese⁴ have discovered the photoreaction where a
31 homolytic fragmentation of a carbon–heteroatom bond is involved, *i.e.*, C-O, C-S and C-N, of esters,
32 thioesters and amides, respectively.⁵ The photo-Fries rearrangement proceeds via a well-established
33 radical mechanism, mainly occurring through the excited singlet state.^{1b,6} Typically, the photoinduced
34 Fries rearrangement reaction of (hetero)aryl benzoates in homogeneous media affords *ortho*- and *para*-
35 regioisomers as well as the corresponding phenols (Scheme 1).^{7,1b}



53 Scheme 1. Photochemistry of aryl benzoates.

The product distribution of the photo-Fries rearrangement underlines the competition between in-cage radical recombination versus out-of-cage diffusion and, consequently, aryl esters, as model substrates, have been chosen to study heterogeneous environments.⁸ In these studies, SDS (sodium dodecyl sulfate) was the preferred surfactant to be tested. In the literature, there are examples of photo-Fries reactions, i.e. irradiation of benzamides in SDS solution and irradiation of aqueous solutions of acetanilides confined in cyclodextrin.^{8b,8d} Recently, we have studied the photo-Fries rearrangement of a variety of substituted acetanilides in micellar solution showing the high selectivity of the photoreaction in favor of the *ortho*-rearranged photoproducts, viz. substituted 2-aminoacetophenones.⁹ The preparation of benzyloxy benzophenone derivatives requires the use of 2-hydroxybenzophenones as key compounds, demonstrating biological activity and pharmaceutical properties (*e.g.* anti-inflammatory and estrogenic activity).¹⁰ Therefore, we carried out the systematic study the photo-Fries rearrangement of a series of *p*-substituted phenyl benzoates in surfactant solutions with the aim to evaluate the selectivity towards the formation of 5-substituted 2-hydroxy benzophenones in constrained environment. Scheme 2 shows the structures of the surfactants as well as the aryl benzoates employed in this systematic study.

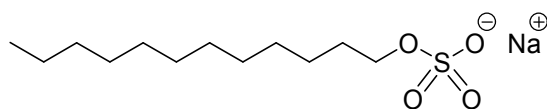
(a) Structures of aryl benzoates.



1 R = OCH₃; 2 R = OPh; 3 R = CH₃; 4; R = *t*-Bu;
5 R = H; 6 R = Ph; 7 R = CN; 8 R = NO₂

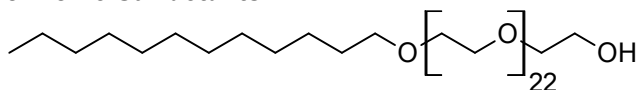
(b) Structures of surfactants.

Anionic Surfactant.



Sodium dodecyl sulfate (SDS)
cmc: 8.2 mM

Non-ionic Surfactants.



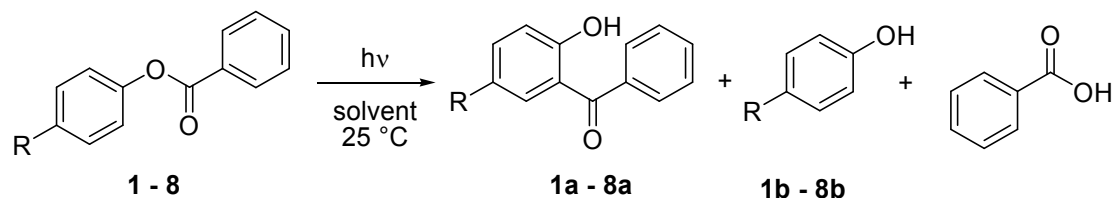
Polyoxyethylene(22)lauryl ether (Brij P35)
cmc: 0.09 mM

Scheme 2. Structures of surfactants and aryl benzoates.

In the present article, we describe the results on the photo-Fries rearrangement of several *para*-substituted aryl benzoates in homogeneous and micro heterogeneous media. The binding constants (K_b) and the location of the substrates within the micelles are measured through spectroscopic methods. From a preparative point of view, the use of anionic and neutral surfactant micelles shows a high selectivity in favor of the formation of the 2-hydroxy benzophenone derivatives achieving yields higher than 90%. From a mechanistic viewpoint, it is furnished the characterization of both *p*-substituted phenoxy radical and substituted 2-benzoylcyclohexadienone transients in homogeneous and micellar environment. The in-cage and out-of-cage rate constants (k_R and k_E , respectively) of *p*-substituted phenoxy radical are measured for the first time by means of laser flash photolysis.

Results.

Steady-state Photolysis. Photoirradiation of aryl benzoates in homogeneous media. Irradiation of aryl benzoates (**1** – **8**) in cyclohexane, MeOH and MeCN which were chosen as representative non-polar, protic polar and aprotic polar solvents, with $\lambda_{exc} = 254$ nm under N_2 atmosphere provided the expected photoproducts from the photo-Fries rearrangement, viz. formation of 2-hydroxybenzophenone derivatives (**1a** – **8a**), the corresponding phenols (**1b** – **8b**) and benzoic acid. The photochemical reaction is depicted in Scheme 3. The formation of benzoic acid was attributed to the oxidation of benzaldehyde, which is the primary photoproduct formed, because of the presence of residual molecular oxygen in the reaction mixture.¹¹ In all the performed reactions, the yield of benzoic acid was between 5 to 15%.



Scheme 3. The photoinduced Fries rearrangement of aryl benzoates (**1** – **8**).

When esters are consumed, the chemical yields collected in Table 1 show that benzophenones **1a** – **8a** are the main photoproducts in up to 94% yield. Furthermore, the product distribution did not change significantly with the nature of the solvent and poor selectivity in favor of the benzophenone derivatives was observed.

Table 1. Irradiation of aryl benzoates in homogeneous solution. Yield of photoproducts,^a reaction quantum yield (ϕ_r)^b and fluorescence quantum yield (ϕ_f)^c.

Aryl benzoates	Solvent	Photoproduct yield (%)		ϕ_r	ϕ_f
		Benzophenones (a)	Phenols (b)		
1	Cyclohexane	46	27	0.30	0.08
	MeCN	62	17	0.36	0.03
	MeOH	66	17	0.33	0.10
2	Cyclohexane	55	28	0.37	0.002
	MeCN	69	19	0.71	0.013
	MeOH	73	23	0.44	0.002
3	Cyclohexane	42	22	0.40	0.25
	MeCN	94	5	0.62	0.07
	MeOH	80	20	0.31	0.11
4	Cyclohexane	59	27	0.50	0.001
	MeCN	95	5	0.35	0.025
	MeOH	75	25	0.63	0.002
5	Cyclohexane	40 ^e	30	0.36	0.001
	MeCN	60 ^e	33	0.14	0.005
	MeOH	58 ^e	26	0.14	0.002
6	Cyclohexane	41	23	0.59	0.012
	MeCN	73	18	0.32	0.035
	MeOH	85	14	0.31	0.033
7	Cyclohexane	38	19	0.51	0.002
	MeCN	84	15	0.82	0.025

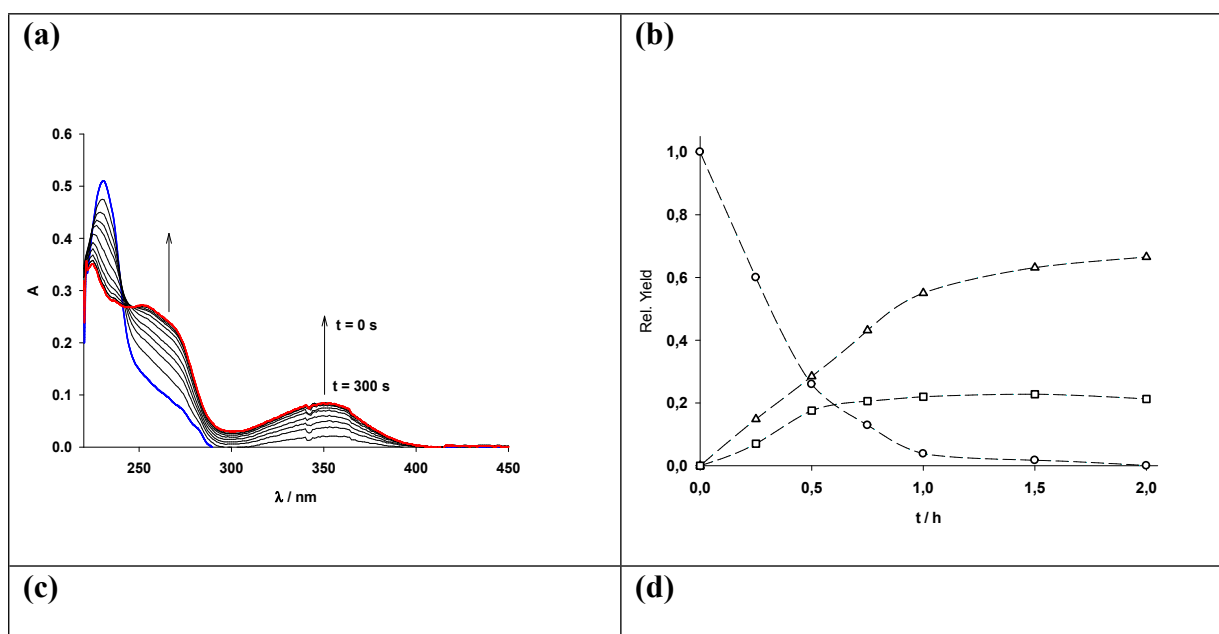
	MeOH	75	26	0.93	0.002
8	Cyclohexane	31	34	0.02	NF ^d
	MeCN	60	40	0.07	NF
	MeOH	50	52	0.07	NF

^a Yield of photoproducts determined by ¹H-NMR spectroscopy in the reaction mixture. Concentration of aryl benzoates: 5.0x10⁻³ M. ^bActinometer: KI (0.6 M), KIO₃ (0.1 M) and Na₂B₂O₇·10H₂O (0.01 M) solution in water; $\phi(I_3^-) = 0.74$; $\lambda_{exc} = 254$ nm.¹²; Error: ± 0.01 . ^cActinometer: 4-chloroanisole acetonitrile solution under Ar atmosphere; $\phi_f = 0.019$ ¹³; Error: ± 0.002 . ^dNF: non-fluorescent substrate. ^e 4-Hydroxybenzophenone is also formed: Cyclohexane 30%; MeCN 7%; MeOH 15%.

The quantum yields of consumption of the aryl benzoates (ϕ_r) in polar and non-polar solvents were measured (see Table 1). The ϕ_r values were found to be higher than 0.30, implying that the photo-Fries rearrangement reaction occurred efficiently. Moreover, in every solvent, a marked increase of the ϕ_r values was observed, moving from esters bearing electron-donor to esters substituted with electron-acceptor substituents. The only exception found was ester **8**. The ϕ_r values measured for compound **8** are lower than 0.10 in all the solvents studied. The aryl benzoates are all poorly fluorescent chromophores (see Table 1) with the exception of benzoate **8** that was found to be non-fluorescent. The spin coupling effect of the nitro group explains the peculiarity of ester **8**.^{14,15} Indeed, intersystem crossing pathway competes with both the photo-Fries rearrangement reaction and the fluorescence emission.

UV-visible and NMR spectroscopies were used to follow the photochemical reaction and aryl benzoates **1**, **2**, **3** and **7** have been chosen as representative examples for such spectroscopic studies. Figure 1(a) showed the time-resolved UV-visible absorption spectrum of the photoreaction of *p*-methylphenyl benzoate (**3**) in cyclohexane showing the growth of a new band located at 352 nm during the irradiation time. This band was assigned to the n,π^* transition of the carbonyl group of benzophenone **3a**¹⁴ and was also observed in MeOH and MeCN. However, no significant solvent effect was observed in the maximum wavelength of the n,π^* transition band upon change of the solvent polarity. A similar solvent effect on the maximum wavelength of the n,π^* band of the 2-hydroxy

1
2 benzophenone derivatives (**1a**, **2a**, **4a** – **8a**) was also observed (see Figure S1 in Supporting
3 Information). On the other hand, a noticeable substituent effect on the n,π^* band of the substituted 2-
4 hydroxy benzophenones (**1a** – **8a**) was observed. In fact, a hypsochromic effect ($\Delta\lambda = -73$ nm) ascribed
5 to the n,π^* band was measured changing the substituent from the electron-donor MeO ($\lambda_{\text{max}} = 378$ nm)
6 to the electron-accepting NO_2 ($\lambda_{\text{max}} = 305$ nm). The course of the photoreaction of ester **1** is detailed in
7 Figure 1(b), where the benzoyl [1;3]-migration to form benzophenone **1a** is shown to be the primary
8 process. Figures 1(c) and 1(d) show the relative formation of benzophenones **2a** and **7a** (starting from
9 the corresponding esters **2** and **7**), respectively, in non-polar and polar solvents. The relative rates of
10 formation of **2a** are similar in MeCN and cyclohexane while in MeOH is somewhat lower implying
11 that in protic polar solvent radiative and non-radiative decay rates compete with the photoreaction
12 pathway. The rates of formation of benzophenone **7a** are quite similar in all the solvents tested. For the
13 other esters studied the relative rates of formation of the corresponding benzophenone derivatives
14 showed a similar behavior (see Figure S2 in Supporting Information).



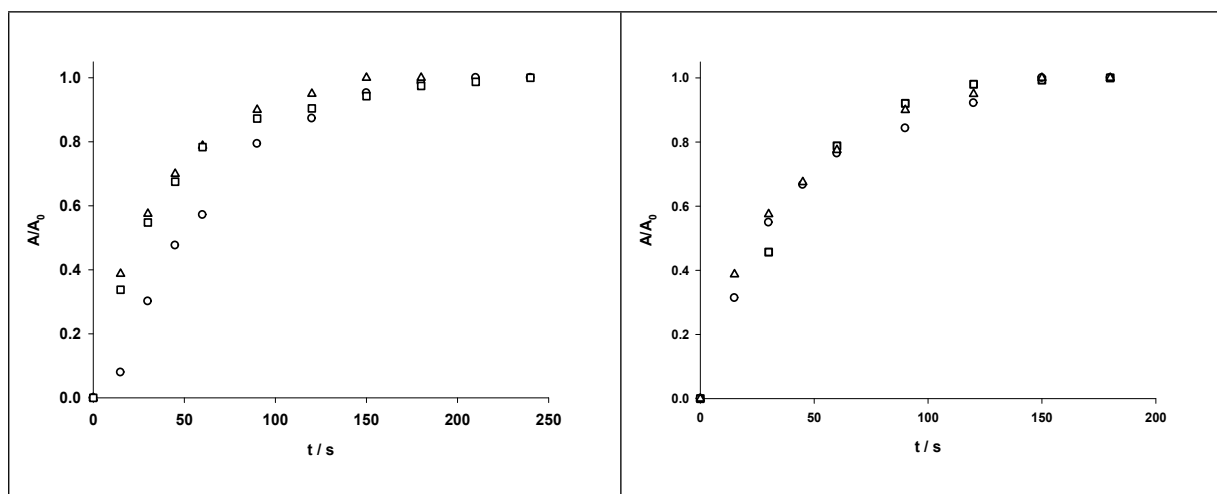


Figure 1. (a) Time-resolved UV-visible absorption spectrum of **3** in cyclohexane. Blue line: initial time; red line: 300 s. (b) Relative yield profile vs time of **1** in MeOH: ester **1** (circles); benzophenone **1a** (triangles); phenol **1b** (square). (c) Relative absorbance at 358 nm (A/A_{∞}) of formation of **2a** in: MeOH (circles); MeCN (triangles); cyclohexane (square). (d) Relative absorbance at 333 nm (A/A_{∞}) of formation of **7a** in: MeOH (circles); MeCN (triangles); cyclohexane (square).

The $^1\text{H-NMR}$ spectra of the photoreaction mixture (6 h irradiation) of 4-cyanophenyl benzoate (**7**) in cyclohexane under N_2 atmosphere were also recorded (see Figure S3 in Supporting Information). As expected, the formation of the photoproducts benzophenone **7a** and phenol **7b** were confirmed through their diagnostic signals (see Figure S3 in Supporting Information) along with the unreacted ester **7**. The experiments demonstrated poor selectivity of the photoreaction in homogeneous media and this trend was observed for all the esters (**1** – **8**) studied (see Table 1).

Photoirradiation of aryl benzoates in micellar media. Irradiation of aryl benzoates (**1** – **8**) in aqueous SDS (0.10 M) with $\lambda_{\text{exc}} = 254$ nm under air caused the selective generation of 2-hydroxybenzophenone derivatives (**1a** – **8a**) in high yields along with lower amounts of the corresponding phenols (**1b** – **8b**) (for structures, refer to Scheme 3). In these experiments consumption up to 95% of aryl benzoates (**1** – **8**) was obtained. The chemical yields of benzophenone derivatives (**1a** – **8a**) are collected in Table 2.

Table 2. Irradiation of aryl benzoates in micellar solution. Yield of 5-substituted-2-hydroxybenzophenones^a and reaction quantum yield (ϕ_r)^b and fluorescence quantum yield (ϕ_f)^c of aryl benzoates.

Benzophenones	Photoproduct yield (%)		ϕ_r		ϕ_f
	SDS	Brij-P35	SDS	Brij-P35	SDS
1a	94	95	0.13	0.12	0.026
2a	76	85	0.79	0.21	0.026
3a	70	92	0.55	0.41	0.024
4a	85	89	0.54	0.26	0.025
5a	90 ^e	92 ^e	0.50	0.21	0.029
6a	87	90	0.53	0.21	0.062
7a	80	78	0.45	0.10	0.024
8a	44	56	0.13	0.01	NF ^d

^a Yield of photoproducts determined by ¹H-NMR spectroscopy in the reaction mixture. Concentration of aryl benzoates: 5.0×10^{-3} M. ^b Actinometer: KI (0.6 M), KIO₃ (0.1 M) and Na₂B₂O₇·10H₂O (0.01 M) solution in water; $\phi(I_3^-) = 0.74$; $\lambda_{exc} = 254$ nm.¹² Error: ± 0.01 . ^c Actinometer: 4-chloroanisole acetonitrile solution under Ar atmosphere; $\phi_f = 0.019$ ¹³; Error: ± 0.002 . ^d NF: non-fluorescent substrate. ^e 4-Hydroxybenzophenone is also formed in 8 – 10%.

As is apparent from Table 2, SDS and Brij-P35 micellar solutions promoted a high selectivity on the photo-Fries rearrangement of the aryl benzoates **2** – **8**, favoring the formation of the corresponding substituted benzophenones (**2a** – **8a**) over the *p*-substituted phenols. The observed selectivity was attributed to the confinement of the aryl benzoates and the radicals formed after the C-O bond cleavage within the hydrophobic core provided by the micellar medium. Moreover, the *p*-substituted phenols were formed in a minor extent or not formed at all, evidencing the suppression of products arising from cage escape. It is worth noticing that the irradiation of *p*-nitrophenyl benzoate (**8**) gave 2-hydroxy-5-nitrobenzophenone (**8a**) only in 44 % yield (the consumption of the starting material was 66 % after 6 h of irradiation). No *p*-nitrophenol was detected in the reaction mixture. Competitive deactivation of the singlet state of *p*-nitrophenyl benzoate (**8**) through intersystem crossing accounted for the observed chemical yield of benzophenone **8a**.¹⁴ The competitive process populates the triplet excited state, due to the spin-orbit coupling provided by the nitro group, which is an unproductive excited state of benzoate **8**.

Quantum yields of consumption of the aryl benzoates (ϕ_r , see Table 2) were measured in micellar media, viz. SDS and Brij-P35, and were found to be of the same order of magnitude. However, the quantum yields measured in SDS solution were larger than in Brij-P35 solutions. This behavior can be attributed to an enhancement of the non-radiative pathway from the singlet state of the aryl benzoates in Brij-P35 solutions. The high-consumption quantum yields and low or no fluorescence emission from aryl benzoates (**1** – **8**) was consistent with a fast reaction from the singlet state. However, non-radiative and intersystem crossing pathways from the singlet state compete with the photo-Fries rearrangement.

UV-visible spectroscopy was used for following the photoreaction and *p*-methoxyphenyl benzoate (**1**) was selected as a representative aryl benzoate. Thus, the reaction of **1** in SDS (0.10 M) was followed by UV-visible absorption spectroscopy and the UV-visible spectral change vs time is shown in Figure 2(a). It is apparent from the UV-visible spectra that the photo-Fries rearrangement of compound **1** to form 2-hydroxy-5-methoxy benzophenone (**1a**) is the primary process, according to the appearance of the characteristic n,π^* band of the carbonyl group located at 372 nm. Similar behavior was observed for compounds **2** – **8** (see Figure S1 in Supporting Information).

The course of the photoreaction of ester **1** is depicted in Figure 2(b) and clearly shows that the benzoyl [1;3]-migration to form benzophenone **1a** is the main process. On the other hand, we selected aryl benzoates **7** and **4** as examples of aryl benzoates to show the relative formation of benzophenones **7a** and **4a**, respectively, in cyclohexane and 0.10 M SDS and 0.01 M Brij-P35 solutions (see Figures 2(c) and 2(d)). The relative rates of formation of **7a** in surfactant media (see Figure 2(c)) are slightly lower than in cyclohexane and can be attributed to the radiative and non-radiative decay rates that compete with the photoreaction pathway. Similar behavior is observed for the rates of formation of benzophenone **4a** (see Figure 2(d)) as well as with for the other benzophenone derivatives (see Figure S2 in Supporting Information).

(a)	(b)
-----	-----

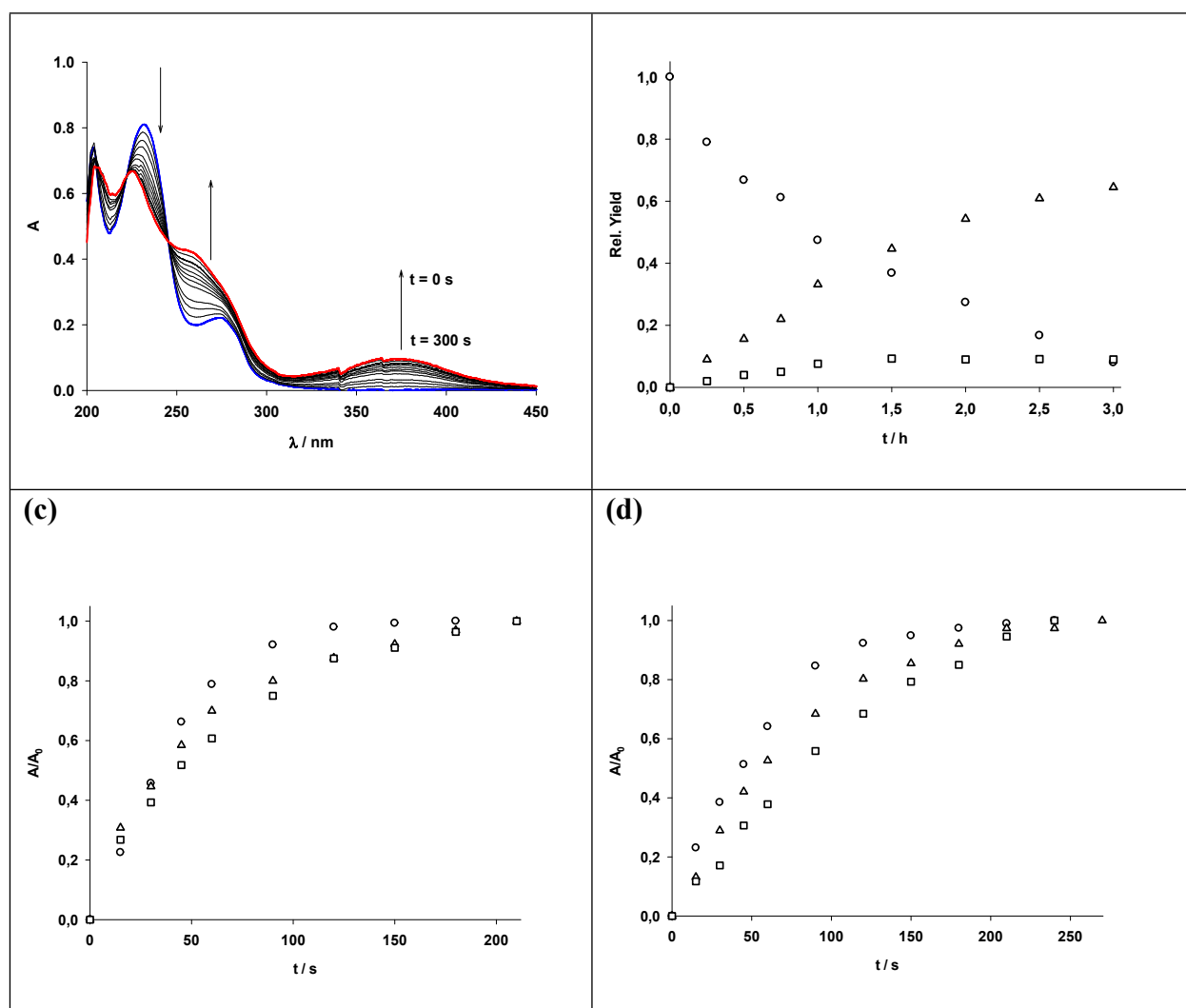
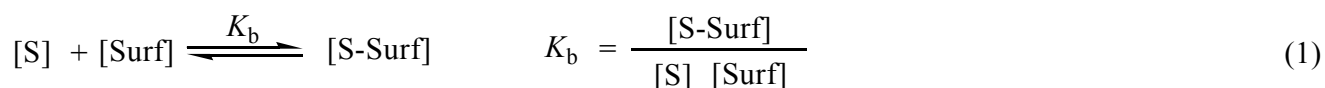


Figure 2. (a) UV-visible spectral change vs time of **1** in SDS 0.10 M in water. Blue line: initial time; red line: 300 s. (b) Relative yield profile vs time of **1** in MeOH: ester **1** (circles); benzophenone **1a** (triangles); phenol **1b** (square). (c) Relative absorbance at 375 nm (A/A_0) of formation of **7a** in: Cyclohexane (circles); 0.10 M SDS solution (triangles); 0.10 m Brij-P35 solution (square). (d) Relative absorbance at 355 nm (A/A_0) of formation of **4a** in: Cyclohexane (circles); 0.10 M SDS solution (triangles); 0.10 m Brij-P35 solution (square).

The photoreaction of compound **1** in micellar environment (SDS 0.10 M) was also followed by NMR spectroscopy. The $^1\text{H-NMR}$ spectra of the reaction mixture of benzoate **1** in SDS (0.10 M) irradiated during 6 h with $\lambda_{\text{exc}} = 254$ nm (see Figure S4 in Supporting Information) showed that benzophenone **1a** was formed in 94 % yield along with *p*-methoxyphenol and benzoic acid in yields lower than 5%. In the same spectra, the signals belonging to the surfactant (SDS) were also observed. The consumption of

benzoate **1** was quantitative. Similar results were obtained with all the aryl benzoates studied (**2 – 8**) and the photoproduct yields are collected in Table 2.

Binding constants (K_b) of aryl benzoates in micellar media. When ionic and neutral surfactant solutions are used as micro reactors to perform photoreactions the knowledge of the reactant's location in the micellar system is required. In order to know the reactant's positioning within micelles, UV-visible and ^1H NMR studies of guest molecules (aryl benzoates) in micellar solution were conducted. UV-visible spectroscopy was used to determine the binding constant (K_b) between micelles and aryl benzoates applying a methodology that have been reported earlier for aryl acetamide.⁹ Both bathochromic and hyperchromic shifts of the lower energy absorption band of the aryl benzoates were observed by addition of increasing amounts of surfactant, demonstrating the binding of the substrates to the micelle that took place within the hydrophobic core of the micelle. Indeed, the binding of the aryl benzoates to the micelle can be described as equilibrium, K_b can be written according to equation 1, where S represents the benzoates, Surf the surfactants and [S-Surf] the complex formed between benzoates and the surfactants.



Equation 2 was obtained after application of Lambert-Beer law on equation 1. A_0 and A are the absorbances at the maximum wavelength in the absence and presence of surfactant, respectively. The molar absorptivity of the complex and the benzoates are dubbed accordingly ϵ_C and ϵ_S . A linear relationship is observed between $(A - A_0)^{-1}$ and the reciprocal of the concentration of the surfactant in equation 3 which was obtained after rearranging equation 2.

$$\frac{(A - A_0)}{A_0} = \frac{\epsilon_C \cdot K_b \cdot [\text{Surf}]}{\epsilon_S \cdot (1 + K_b \cdot [\text{Surf}])} \quad (2)$$

$$\frac{A_0}{(A - A_0)} = \frac{\epsilon_S}{\epsilon_C} + \frac{\epsilon_S}{\epsilon_C \cdot K_b} \frac{1}{[\text{Surf}]} = A_0 \frac{1}{\Delta A} \quad (3)$$

The experimental data obtained for some aryl benzoates and SDS and Brij-P35 are shown in Figure 3 and the best linear regression curves are also included in the same figure. The plots for the other systems are collected in Figure S5 (see Supporting Information). The K_b values for **1** – **8** calculated from the ratio between the slope and the intercept of the regression curve are shown in Table 3. From these data it is apparent that the benzoates bind to the micelles and the ones possessing hydrophobic character, i.e. benzoates **1** and **4** in SDS micellar solution, show high K_b values. Likewise, benzoates **1**, **4** and **7** possess greater K_b compared to the other substrates in the case of Brij-P35 micellar solution. Generally, the K_b values obtained for benzoates **1** – **8** are typical of aromatic solutes as it pointed out by Quina, Treiner and co-workers.¹⁶ Estimation of K_b values $\leq 100 \text{ M}^{-1}$ in SDS for weakly hydrophobic substrates such as phenyl chloroformate have also been reported.¹⁷ Likewise, K_b values have been reported for the binding of Brij-P35 surfactant and a series of benzoyl chloride derivatives and they were found to be higher than those obtained for other surfactants such as SDS and CTAC.¹⁸ Estimation of a minimum value around 190 M^{-1} for the binding constant (K_b) of Brij-P35 surfactant was reported and accounts for a more apolar environment when pyrene was used as a micropolarity probe.¹⁸

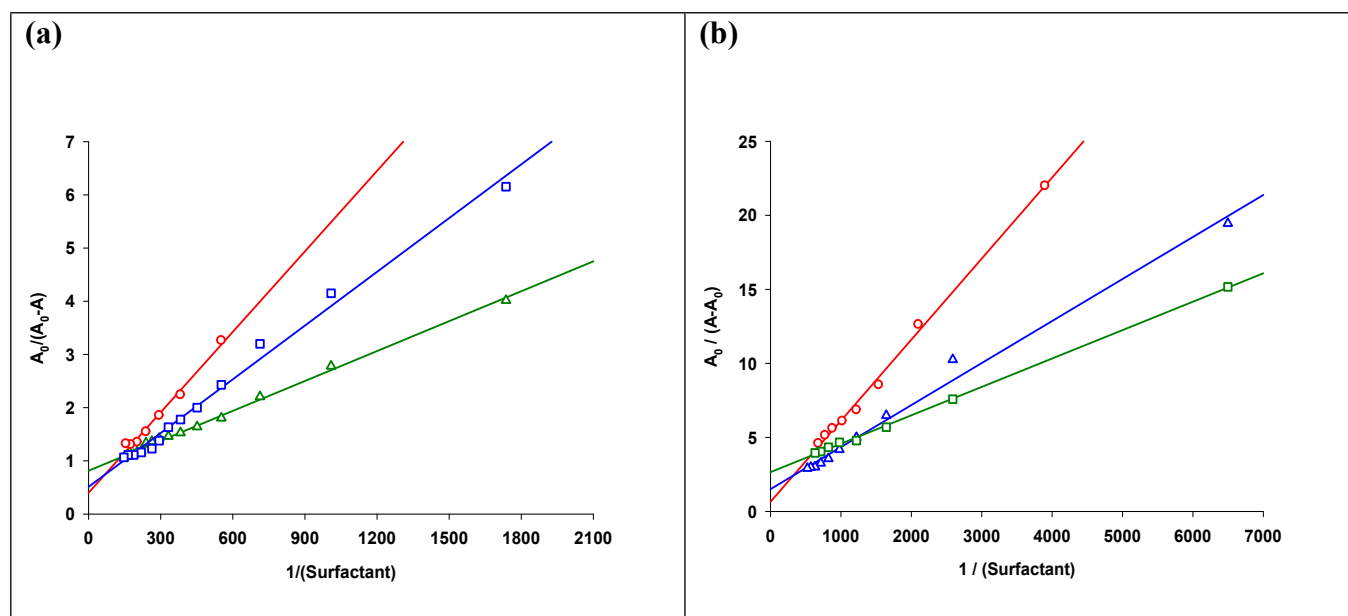


Figure 3. Reciprocal plotting ($(A_0/(A-A_0))$ vs concentration of surfactants) in water at room temperature: (a) SDS (circles: **2**; squares: **4**; triangles: **7**) and (b) Brij-P35 (circles: **2**; squares: **4**; triangles: **1**). In all the linear fitting regressions: $r^2 > 0.99$.

Table 3. Binding constant (K_b) in water of surfactants (SDS and Brij-P35) and aryl benzoates.

Aryl benzoates	K_b / M^{-1}							
	1	2	3	4	5	6	7	8
SDS	1402	80	127	539	42	10	18	74
Brij-P35	1398	581	69	423	63	26	1394	181

2D NMR spectroscopy has been recorded to confirm qualitatively the location of the aryl benzoates within the micelle. NOESY experiments have been often used to determine the localization of substrates inside the micelle as well as to determine the extent of co-aggregation between two different kinds of surfactants in water.¹⁹ Positive results are achieved when cross-peaks between diagnostic signals of the substrate and the surfactants, respectively, are observed in the corresponding contour plots.⁹ Thus, the NOESY experiments were performed in D₂O and Figure 4 shows the 2D NMR spectrum for a solution of SDS (7 mM) in the presence of benzoate **1** (10 mM). The inset red frames recognize the NOE (Nuclear Overhauser Effect) between the signals of the surfactant SDS (bulk hydrogens and α hydrogen) and the signals belonging to the aromatic protons (H-2/H-6, H-3/H-5, H-10/H-14, H-12 and H-12/H-13) of *p*-cyanophenyl benzoate **7**. Also, Figure 6 shows the labels of the protons of the surfactant SDS and the aryl benzoate **7**, respectively. Similar spectroscopic behavior was observed for solutions of SDS and Brij-P35 in D₂O in the presence of aryl benzoates **1** and **3** (see Figures S6, S7 and S8 in Supporting Information). The cross-peaks of diagnostic signals observed in the 2D NMR contour plots are in agreement with and reinforce the UV-visible spectroscopic analyses.

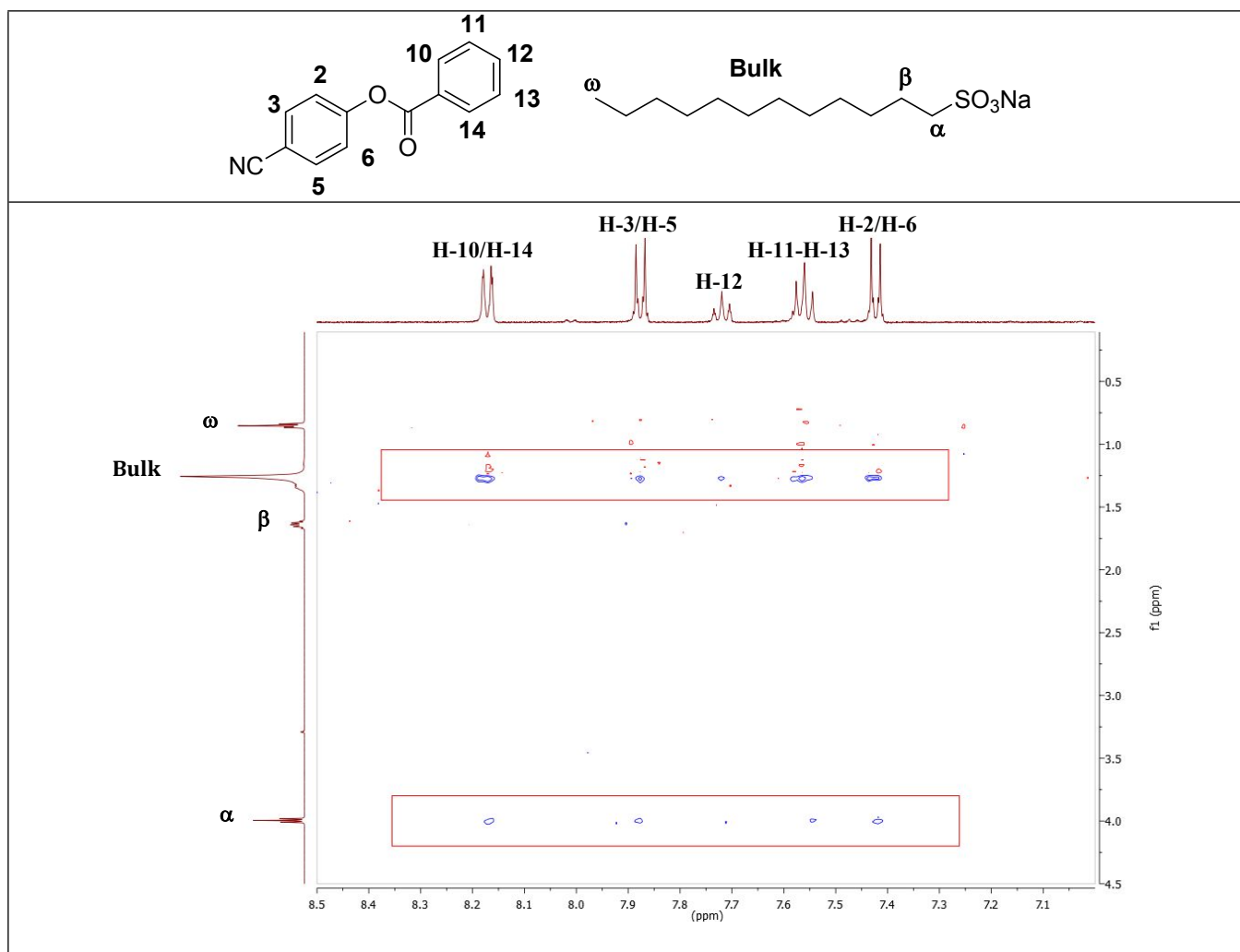
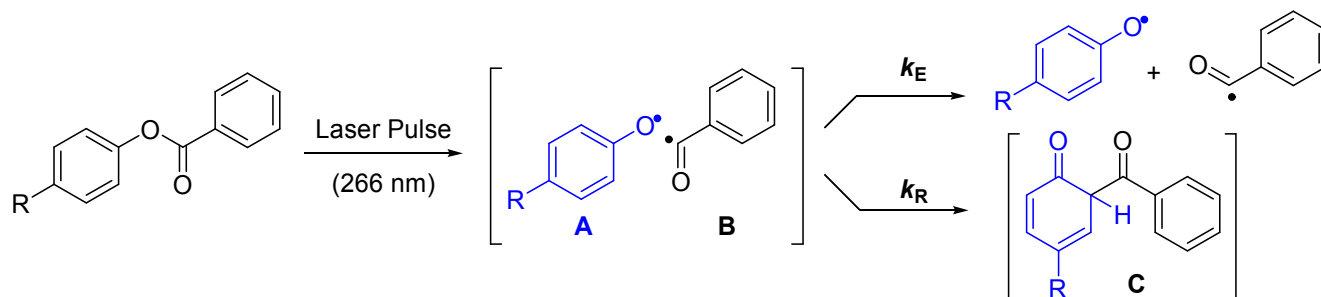


Figure 4. 2D NOESY contour plot of a solution of SDS (7 mM) and **7** (10 mM) in D₂O at room temperature.

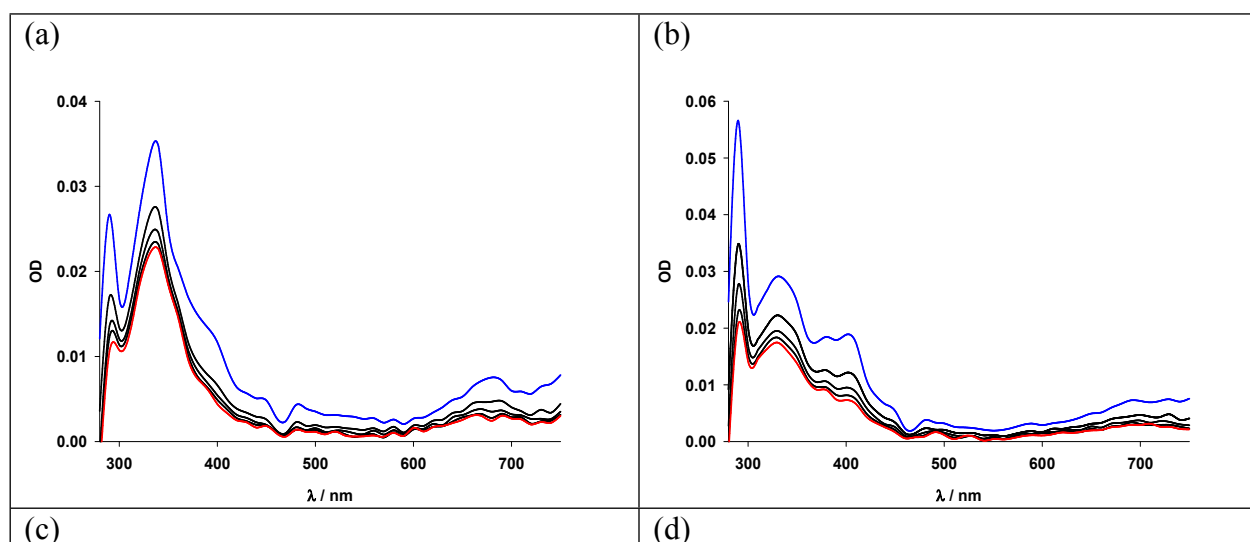
However, we cannot estimate the location of the benzoates with accuracy but we can suggest that the benzoates are located inside the hydrophobic core of the micelle because the proton nuclei of the aryl benzoates correlate nicely with the proton nuclei of the surfactants as can be seen through the cross-peaks of the contour plots.

Laser Flash photolysis of aryl benzoates. Irradiation of *p*-methoxyphenyl benzoate (**1**) in acetonitrile and cyclohexane solutions with a laser pulse (266 nm) under nitrogen atmosphere gives the transient absorption spectra shown in Figures 5(a) and (b). Four absorption bands with maximum wavelength at 290, 340, 400 and 720 nm were observed in the transient spectra. According to the data reported in the literature, we attributed the bands located at 290 nm and 400 nm to the *p*-methoxyphenoxy radical

while those bands centred at 340 nm and 720 nm were attributed to cyclohexadienone transient.²⁰ Two consecutive pathways from the singlet excited state of ester **1** are involved in the formation of both transients after the pulse (266 nm): (i) homolytic fragmentation of the C-O bond of the ester group affording *p*-methoxyphenoxy and benzoyloxy radical species in the solvent cage (intermediates **A** and **B**, respectively, in Scheme 4), and then, (ii) coupling of both radical species to give the 4-methoxy-2-benzoylcyclohexadienone intermediate (**C** in Scheme 4). Also, in Figures 5(c) and (d) are reported the transient absorption spectra of compounds **6** and **2** in acetonitrile after the laser pulse (266 nm). Two characteristic bands located around 340 and 400 nm are observed which were assigned to the substituted 2-benzoylcyclohexadienone and substituted phenoxy radical intermediates, respectively. Noteworthy similar results are obtained for the other aryl benzoates studied (see Figure S9 in Supporting Information).



Scheme 4. Formation of transient species after the laser pulse (266 nm).



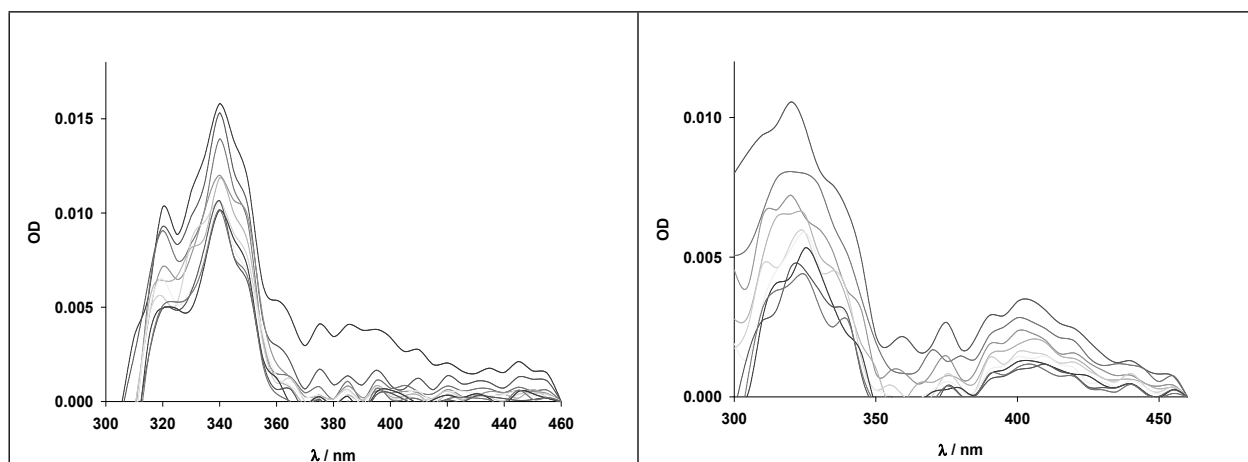
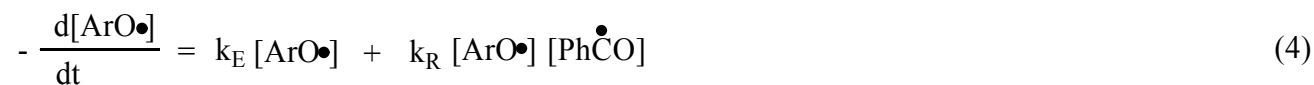
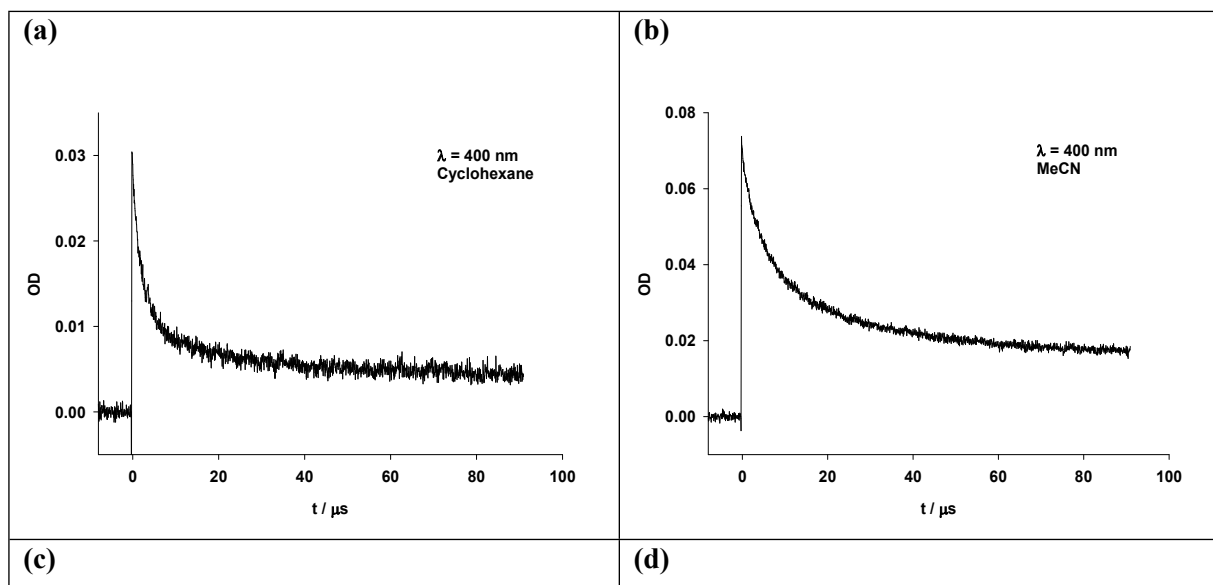


Figure 5. Transient absorption spectra obtained after a laser pulse (100 μ s; λ_{exc} : 266 nm) of solutions (5.1×10^{-4} M) of: (a) **1** in cyclohexane; (b) **1** in acetonitrile; (c) **6** in acetonitrile and (d) **2** in acetonitrile under nitrogen atmosphere.

The decay traces of the transient signal assigned to 4-substituted phenoxy radicals were also measured at 400 nm in N_2 -saturated cyclohexane and acetonitrile solutions (after a laser pulse at 266 nm). The experiment was done with the aim of determining both the rate constants of radical out-of-cage escape (k_E) and *ortho* coupling reaction (k_R) (see Scheme 4). Some selected examples of the decay traces are shown in Figure 6. The decay traces of 4-substituted phenoxy radicals show biexponential decay fitting with r^2 values > 0.998 independent of the solvent used. Two half lifetime values were obtained from the nonlinear fittings, τ_E and τ_R : the short lifetime (τ_R) was assigned to in-cage coupling process while the large lifetime (τ_E) was assigned to the phenoxy radical out-of-cage process by comparison with earlier reported data regarding thiyl radicals.^{20e,21} This biexponential behaviour can be interpreted considering the two competitive pathways the 4-substituted phenoxy radical can undergo, viz. out-of-cage escape and in-cage coupling pathways, (see Scheme 4). This behavior can be described according to equation 4 where ArO^\bullet represents the substituted phenoxy radical and PhCO^\bullet represents the benzoyl radical.



The out-of-cage escape of the substituted phenoxy radical is a unimolecular pathway. Therefore, the rate constant (k_E) of this process can be calculated from the reciprocal of the lifetime, $k_E = 1 / \tau_E$ (see Table 4). The in-cage coupling rate constants (k_R) were obtained by plotting the reciprocal of the concentration of the substituted phenoxy radicals against time and excellent linear correlations were observed (see Figure S11 in Supporting Information for the linear correlations). Then, after applying a linear regression fitting the in-cage coupling rate constants (k_R) were obtained from the slopes and these data are also shown in Table 4. As can be seen in Table 4, it is apparent that the out-of-cage rate constants (k_E) for the unimolecular escape process of 4-substituted phenoxy radicals are quite similar in all the solvents studied (1.5 to $8.3 \times 10^5 \text{ s}^{-1}$) and somewhat independent of the substituent. On the other hand, the bimolecular in-cage coupling of 4-substituted phenoxy and benzoyl radicals was found to be a second-order rate constant (k_R) of $10^9 - 10^{10} \text{ M}^{-1} \cdot \text{s}^{-1}$ in N_2 -saturated solvents with no significant substituent effect associated to it.



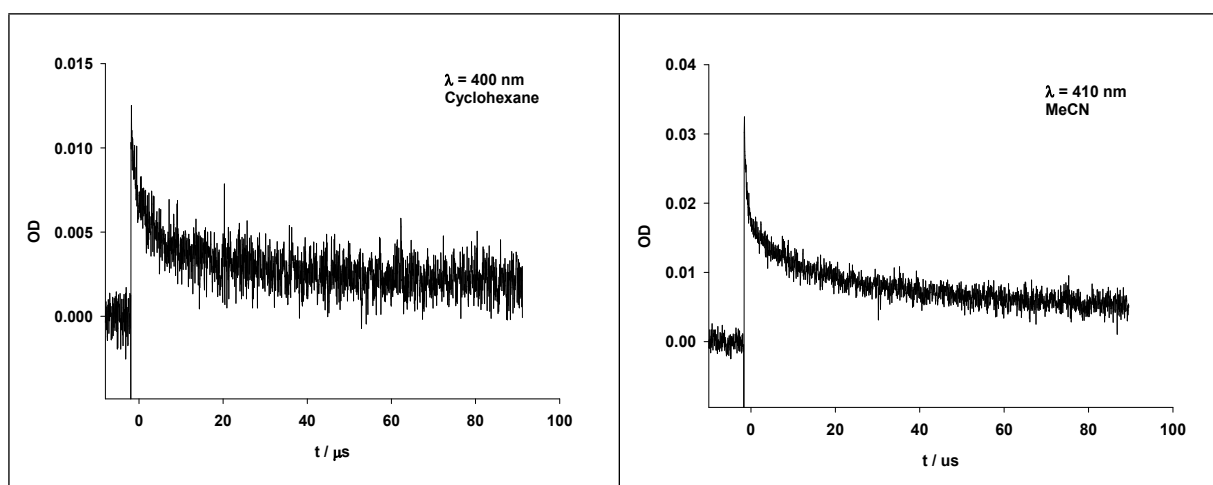
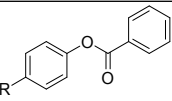


Figure 6. Decay traces of 4-substituted phenoxy radical recorded at 400 nm after the laser pulse (λ_{exc} : 266 nm) of solutions (5.1×10^{-4} M) of: (a) 4-methoxyphenyl benzoate (**1**) in cyclohexane; (b) 4-methoxyphenyl benzoate (**1**) in acetonitrile; (c) 4-tert-butylphenyl benzoate (**4**) in cyclohexane; (d) 4-phenoxyphenyl benzoate (**2**) in acetonitrile under N_2 atmosphere.

Table 4. Out-of-cage (k_E) and in-cage coupling (k_R) rate constants of 4-substituted phenoxy radicals measured by laser flash photolysis (266 nm) in different solvents under N_2 atmosphere.^a

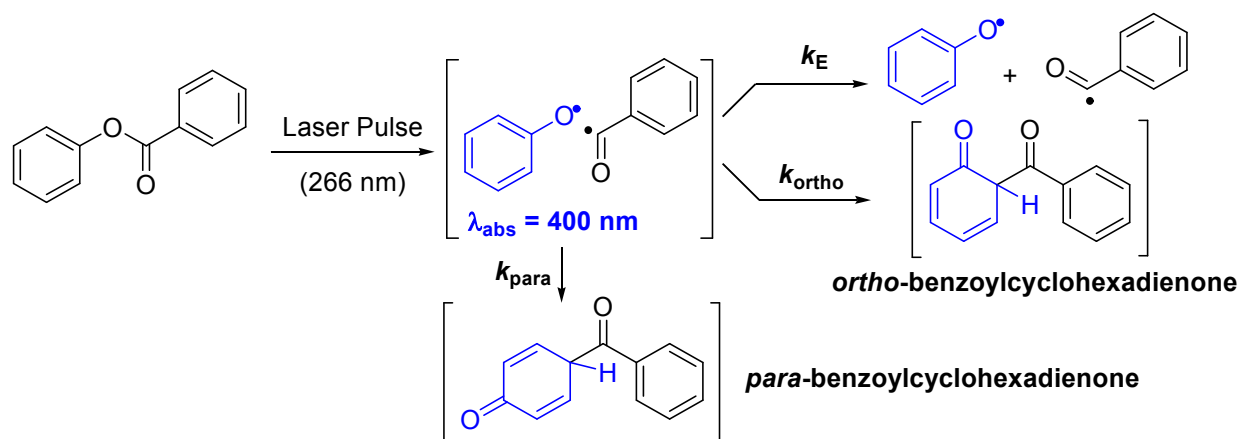
Rate constants							
	MeCN		MeOH		Cyclohexane		SDS (0.10 M)
	$k_E \times 10^{-5} / \text{s}^{-1}$	$k_R \times 10^{-9} / \text{M}^{-1} \cdot \text{s}^{-1}$	$k_E \times 10^{-5} / \text{s}^{-1}$	$k_R \times 10^{-9} / \text{M}^{-1} \cdot \text{s}^{-1}$	$k_E \times 10^{-5} / \text{s}^{-1}$	$k_R \times 10^{-9} / \text{M}^{-1} \cdot \text{s}^{-1}$	$k_R \times 10^{-9} / \text{M}^{-1} \cdot \text{s}^{-1}$
R							
OMe (1)	2.2±0.1	5.5±0.1	2.8±0.1	15±1	4.5±0.1	8.9±0.1	3.9±0.1
OPh (2)	8.3±0.2	14±1	1.0±0.2	24±1	2.2±0.2	46±1	25±1
Me (3)	3.0±0.1	1.4±0.1	6.7±0.1	1.7±0.1	2.5±0.1	7.3±0.1	3.0±0.1
t-Bu (4)	1.5±0.1	28±1	3.4±0.1	12±1	3.4±0.1	3.4±0.1	26±1
Ph (6)	5.0±0.2	4.6±0.1	1.0±0.2	6.1±0.1	Insoluble		1.2±0.1
CN (7)	4.8±0.2	9.5±0.1	2.3±0.2	9.9±0.1	1.3±0.2	36±1	17±1

^a Concentration of aryl benzoates: 5.0×10^{-4} M.

A similar spectroscopic analysis was carried out with aryl benzoates in aqueous SDS (0.10 M) solutions after irradiation with a pulse at 266 nm. Two characteristic bands (340 – 360 nm and 400 nm) are observed in the transient absorption spectra and 4-substituted phenoxy radicals showed second order kinetic decay traces. The in-cage coupling rate constants (k_R) were obtained by plotting the

reciprocal of the concentration of the 4-substituted phenoxy radicals against time and, after applying a linear regression fitting, the rate constants (k_R) were obtained from the slopes (see Table 4). No significant substituent effect on the rate constants (k_R) was observed when the solvent was a micellar solution (SDS 0.10 M) which gave a similar trend that was observed in homogeneous media.

Because phenyl benzoate (**5**) has no substituent in *para* position, two possible *ortho*- and *para*-benzoylcyclohexadienone regioisomers can be proposed (see Scheme 5). Therefore, we have recorded the transient absorption spectra and transient decay traces of compound **5** in different N_2 -saturated solvents with a laser pulse at 266 nm systematically. Figure 7(a) shows both the transient absorption spectra and decay trace recorded at 400 nm in MeCN. The band located at 400 nm in the transient absorption spectra was assigned to the phenoxy radical while the large structured band located between 330 and 385 nm was assigned to *ortho*-benzoylcyclohexadienone and *para*-benzoylcyclohexadienone transients (see Scheme 5).



Scheme 5. Formation of transient species after the laser pulse (266 nm) from phenyl benzoate.

On the other hand, Figure 7(b) shows the decay trace of phenoxy radical measured at 400 nm in N_2 -saturated acetonitrile solution after the laser pulse (266 nm). Biexponential decay was observed after a non-linear fitting. This biexponential behaviour can be interpreted considering the competitive pathways the phenoxy radical can take viz. out-of-cage escape and *ortho* and *para* in-cage coupling

pathways (see Scheme 5). The rate constant (k_E) of the out-of-cage escape pathway was calculated from the reciprocal of the lifetime, $k_E = 1/\tau_E$. The rate constants thus obtained are shown in Table 5. In addition, the *ortho* and *para* in-cage coupling constants, k_{ortho} and k_{para} , were obtained by plotting the reciprocal of the concentration of the phenoxy radical against time and two nice linear correlations were observed (see Figure S12 Supporting Information for the linear correlations). Then, after applying a linear regression fitting to the linear correlations, the in-cage coupling constants were obtained from the slopes and these data are also shown in Table 5. No significant solvent effect on the rate constants was observed. However, the in-cage *para*-coupling pathway is rather lower than the *ortho*-coupling pathway.

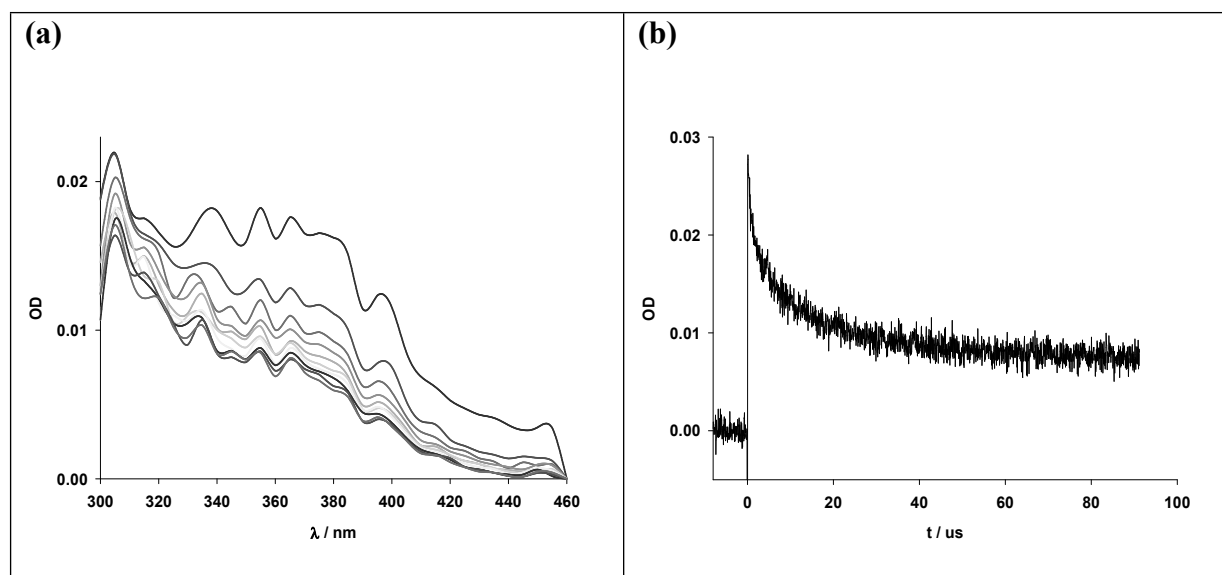


Figure 7. (a) Transient absorption spectra of phenyl benzoate (**5**) recorded in N₂-saturated acetonitrile solution (5.1×10^{-4} M) and (b) decay trace of phenoxy radical recorded at 400 nm after the laser pulse (100 μs; λ_{exc} : 266 nm) of N₂-saturated acetonitrile solution (5.1×10^{-4} M) of phenyl benzoate (**5**).

Table 5. Out-of-cage (k_E) and in-cage coupling (k_{ortho} and k_{para}) rate constants of phenoxy radicals measured by laser flash photolysis (266 nm) in different solvents under N₂ atmosphere.^a

Solvents	Rate constants		
	$k_E \times 10^{-5} / s^{-1}$	$k_{ortho} \times 10^{-9} / M^{-1} \cdot s^{-1}$	$k_{para} \times 10^{-9} / M^{-1} \cdot s^{-1}$
Cyclohexane	4.8 ± 0.1	8.7 ± 0.1	4.1 ± 0.1

MeCN	4.8±0.1	8.4±0.1	3.2±0.1
MeOH	3.1±0.1	2.7±0.1	1.4±0.1
SDS (0.10 M)	---	5.5±0.2	1.5±0.2

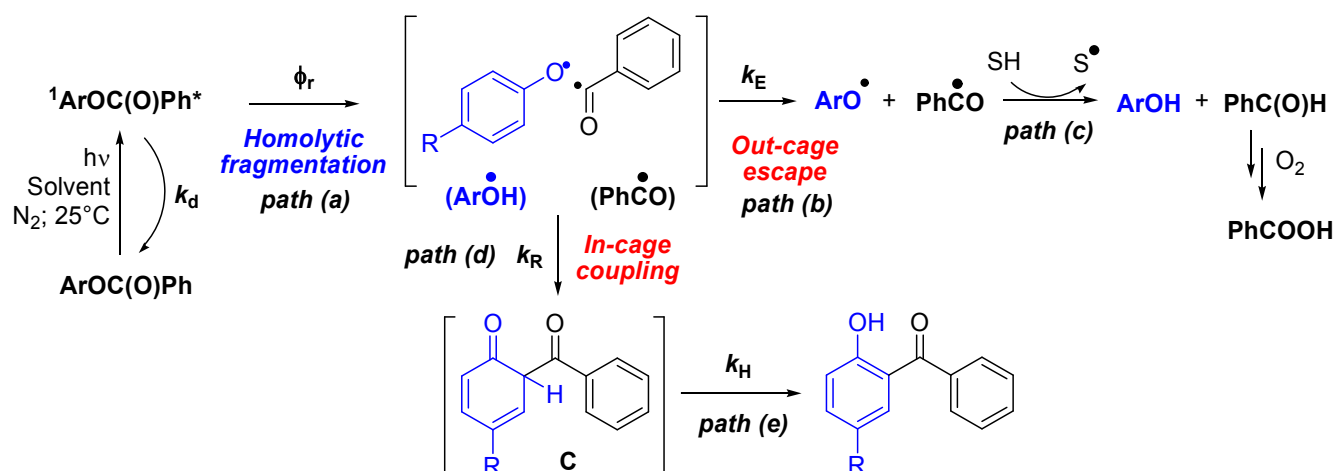
^a Concentration of phenyl benzoates: 5.0x10⁻⁴ M.

Discussion.

As it was described above, direct irradiation (254 nm) of aryl benzoates in homogeneous media (cyclohexane, MeCN and MeOH) as well as in micro heterogeneous media (SDS and Brij-P35 aqueous solutions) under N₂ atmosphere took place efficiently (see Figures 1 and 2). During the irradiation of aryl benzoates a noticeable selectivity in favour of the benzophenone derivatives was observed in micellar media. In this case, the formation of the corresponding substituted phenols was lower than 2 % because of the confined hydrophobic core of the micelle (compare the data shown in Tables 1 and 2). The reaction mechanism depicted in Scheme 6 was sustained by the results obtained under steady-state conditions and laser flash photolysis experiments. When aryl benzoates are irradiated at 254 nm, population of the singlet state is achieved efficiently. This excited state is the photo reactive state of the photoreaction as it was reported in the literature.⁵ Two pathways are involved in the deactivation of the singlet state, (i) homolytic fragmentation of the C-O bond (*path (a)*; Scheme 6) affording aryl phenoxy (ArO•) and benzoyl (PhCO•) radicals that evolves to 5-substituted-2-hydroxybenzophenone and 4-substituted phenol and (ii) photophysical deactivation (*k_d*; Scheme 3) of the singlet state involving fluorescence emission and internal conversion pathways that give the aryl benzoates in their ground state. In the case of ester **8**, intersystem crossing pathway must be considered as a process involved in the physical deactivation pathway estimating a ϕ_T value around 0.50.^{14,15} Irradiation of aryl benzoates in N₂-saturated solutions with a laser pulse ($\lambda_{exc} = 266$ nm) gave the transient absorption of 4-substituted phenoxy radical and 5-substituted-2-benzoylcyclohexadienone and these transients were formed immediately at 10 μ s after the incident light (see, for example, Figure 5 for compounds **1**, **2** and

6) demonstrating that C-O homolytic fragmentation (*path (a)* in Scheme 6) and in-cage coupling pathway (*path (d)* in Scheme 6) occurred efficiently.

The decay traces of the phenoxy radical transients were obtained at 400 nm in homogeneous media under inert atmosphere and biexponential decay was observed. Second-order kinetics (k_R) of 10^9 to 10^{10} $M^{-1}.s^{-1}$ were obtained (see Table 4 and Figure 6) and were attributed to the in-cage coupling of the substituted phenoxy radical and benzoyl radical (*path (d)* in Scheme 6) providing the substituted 2-benzoylcyclohexadienone intermediates **C**. These last intermediates, i.e. intermediates **C**, are long-lived species showing lifetime values higher than 200 μs . The [1;3]-hydrogen migration and aromatization reaction pathway (*path (e)* in Scheme 6) were estimated to occur with first-order kinetics (k_H) lower than 5×10^3 s^{-1} providing the substituted 2-hydroxybenzophenone derivatives as the main photoproducts (see Table 1). On the other hand, first-order kinetics (k_E) of 10^5 s^{-1} were also obtained (see Table 4) which were assigned to the escape of the phenoxy radical from the solvent cage (*path (b)* in Scheme 6) that in turn evolved to the 4-substituted phenol by abstraction of hydrogen from the reaction solvent (*path (c)* in Scheme 6; SH: solvent).

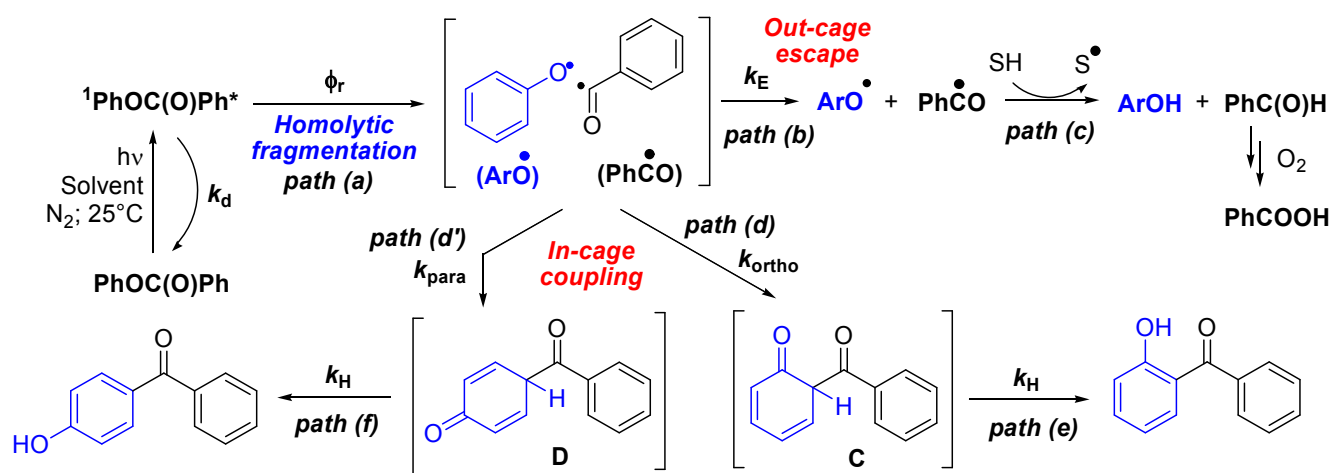


Scheme 6. The reaction mechanism for the irradiation of aryl benzoates with $\lambda_{exc} = 254$ nm.

1
2 Second-order rate constants (k_R) in the range of 10^9 to $10^{10} \text{ M}^{-1} \cdot \text{s}^{-1}$ were obtained (see Table 4) from the
3
4 fitting analysis of the decay traces of the phenoxy radicals measured at 400 nm in micellar media (SDS
5
6 and Brij-P35) under N_2 atmosphere. These values describe the in-cage coupling within the core of the
7
8 micelle of the substituted phenoxy radical (ArO^\bullet) and benzoyl radical (PhC(O)^\bullet) (see *path (d)* in
9
10 Scheme 6). This pathway afforded the substituted 2-benzoylcyclohexadienone intermediates **C**, also
11
12 formed within the hydrophobic core of the micelle, that evolved through a [1;3]-hydrogen migration
13
14 and aromatization reactions to substituted 2-hydroxybenzophenone. Because intermediates **C** are also
15
16 long-lived species in micellar media ($\tau > 200 \mu\text{s}$) the rate constants k_H were estimated to be lower than
17
18 $5 \times 10^3 \text{ s}^{-1}$ as it was observed in homogeneous media.
19
20
21

22
23 It is worth to mention that the only photoproducts detected in micellar media were the 2-
24
25 hydroxybenzophenone derivatives **1a** – **8a** formed with chemical yields up to 95 % (see Table 2) the
26
27 yield of substituted phenols were lower than 5 %. Therefore, we suggest that the escape of the phenoxy
28
29 radical from the hydrophobic core of the micelle (*path (b)* in Scheme 6) is not a productive pathway.
30
31 The decay traces of phenoxy radicals in micellar media did not show biexponential decay traces as it
32
33 was observed in homogeneous media but second-order kinetics that is in agreement with the in-cage
34
35 coupling pathway (*path (d)* in Scheme 6).
36
37

38
39 Additional comments about the irradiation of phenyl benzoate (**5**) in homogeneous and micellar media
40
41 are needed. The results obtained under steady-state conditions and time-resolved spectroscopy on
42
43 phenyl benzoate led us to advance the different reaction pathways depicted in Scheme 7. Irradiation of
44
45 phenyl benzoate populated the singlet excited state efficiently and competitive physical deactivation
46
47 (k_d) and homolytic fragmentation (*path (a)* in Scheme 7) pathways occurred.
48
49
50
51
52
53
54
55
56
57
58
59
60



Scheme 7. Proposed reaction mechanism for direct irradiation of phenyl benzoate (5).

After fragmentation phenoxy and benzoyl radical species were formed in the solvent cage, then, escape of the radical species from the solvent cage (*path (b)*) and hydrogen abstraction from the solvent (*path (c)*) gave the conventional products. Laser flash photolysis experiments provided rate constants (k_E) in cyclohexane, MeCN and MeOH (see Table 5) following the decay trace of phenoxy radical at 400 nm. No escape of the radical species was detected in micellar solution. Because phenyl benzoate has no substituent in *para* position, two possible *ortho*- and *para*-benzoylcyclohexadienone regioisomers viz. intermediates **C** and **D** were formed through the in-cage coupling of the radical species (*path (d)*) and *path (e)* in Scheme 7). Both intermediates **C** and **D** were observed in the absorption transient spectra (see Figure 7) with characteristic bands located in the range of 340 – 380 nm. Besides, the k_{ortho} and k_{para} values in the order of $10^9 \text{ M}^{-1}\cdot\text{s}^{-1}$ belonging to in-cage coupling pathways (*paths (d)* and (*d'*) in Scheme 7) implied that the coupling reaction occurred efficiently in all the solvents studied. Then, intermediates **C** and **D** formed in the solvent cage evolved to the regioisomers 2-hydroxybenzophenone and 4-hydroxybenzophenone through the sequence [1;3]-hydrogen migration and aromatization pathways (*path (e)* and *path (f)* in Scheme 7). Again, intermediates **C** and **D** showed lifetimes higher than 200 μs and the rate constants k_H was estimated to be lower than 10^3 s^{-1} . These photoproducts were

1
2 formed with 30 – 60 % yields together with the corresponding phenol in homogeneous media (see
3
4 Table 1) while in micellar solution were formed in up to 95 % yield and no phenol was detected in the
5
6 micellar reaction mixture.
7

11 **Conclusions.**

12
13 The photochemical reaction of aryl benzoates examined in this paper takes place efficiently in
14
15 homogeneous and micellar media. High selectivity in the formation of the 5-substituted-2-
16
17 hydroxybenzophenone derivatives was observed in micellar media providing these photoproducts in
18
19 yields up to 95 % without the formation of the corresponding phenols. Location of the aryl benzoates
20
21 with 2D NOESY NMR spectroscopy in the shell or in the hydrophobic core of the micelle and
22
23 measurement of the binding constants (K_b) between the benzoates and the surfactants account for the
24
25 selective behaviour observed where diffusion of the radical species from the micelle is inhibited. On
26
27 the other hand, benzophenone derivatives, as the main photoproducts, and the *p*-substituted phenols
28
29 were formed when the irradiations were carried out in homogeneous media such as cyclohexane,
30
31 MeCN and MeOH but no selectivity was observed.
32
33
34
35

36 Laser flash photolysis led to characterize two intermediates viz. the substituted phenoxy radical and the
37
38 5-substituted-2-benzoylcyclohexadienone transients. These intermediates were formed in the cage
39
40 solvent within 10 μ s after the laser pulse. Also, the phenoxy radical escapes from the solvent cage with
41
42 first-order rate constants (k_E) of 10^5 s⁻¹ that in turn evolve to the corresponding phenols by hydrogen
43
44 abstraction from the reaction solvent (see Schemes 6 and 7). The kinetic parameters (k_R) for in-cage
45
46 coupling pathways of the radical species viz. substituted phenoxy and benzoyl radicals were also
47
48 measured in all the solvents studied, providing the corresponding 5-substituted-2-
49
50 benzoylcyclohexadienone intermediates (intermediate **C** in Scheme 6 and intermediates **C** and **D** in
51
52 Scheme 7). These species which are formed in the solvent cage evolved to the regioisomeric 5-
53
54 substituted 2-hydroxybenzophenone derivatives through the sequence [1,3]-hydrogen migration and
55
56
57
58
59
60

1
2 aromatization pathways (*path (e)* in Scheme 6 and *paths (f)* in Scheme 7). Because, these intermediates
3
4 showed lifetimes higher than 200 μs the rate constants k_{H} were estimated to be lower than 10^3 s^{-1} in all
5
6 the solvents studied.
7

8
9 Finally, the finding that the selectivity observed in the photo-Fries rearrangement of some aryl
10
11 benzoates in green and sustainable micellar media gives 5-substituted-2-hydroxybenzophenone
12
13 derivatives in yields up to 95 % could be applied in the preparation of a new wide variety of
14
15 substituted-2-hydroxybenzophenone derivatives.
16
17

18 19 20 **Experimental.**

21
22 *Materials and equipment.* *p*-Substituted phenols, benzoyl chloride, pyridine, sodium dodecyl sulfonate
23
24 and Brij-P35 were obtained from commercial sources. Spectroscopic grade solvents were used as
25
26 received. Pyridine was distilled and stored over KOH pellets. Melting Points were determined with a
27
28 Fisher Jones apparatus and are not corrected. ^1H and ^{13}C NMR spectra were recorded in CDCl_3 on a
29
30 300 MHz spectrometer; chemical shifts (δ) are reported in part per million (ppm), relative to signal of
31
32 tetramethylsilane, used as internal standard. 2D NOESY spectra were recorded in D_2O on a 500 MHz
33
34 spectrometer, using NOESY-ph pulse sequence with a 600 ms mixing time and a recovery delay of 1.5
35
36 s. 2K data points were collected for 512 increments of 16 scans, using TPPI f1quadrature detection;
37
38 chemical shifts (δ) are reported in part per million (ppm), relative to the signal of
39
40 trimethylsilylpropionic acid, used as internal standard. Coupling constant (J) values are given in Hz.
41
42 The measurements were carried out using standard pulse sequences. GC analysis was carried out on a
43
44 Hewlett Packard 5890 gas chromatograph using an Ultra 2 capillary chromatographic column. The
45
46 chromatograms were recorded with the following program: *initial temperature*: 100 $^\circ\text{C}$, 2 minutes;
47
48 *gradient rate*: 10 $^\circ\text{C}\cdot\text{min}^{-1}$; *final temperature*: 250 $^\circ\text{C}$, 10 minutes. The UV-visible spectra were
49
50
51
52
53
54
55
56
57
58
59
60

1
2 measured with a Shimadzu UV-1203 spectrophotometer using two-faced stoppered quartz cuvettes (1
3 mm x 1 mm) at 298 K.

4
5
6 *Determination of the binding constants (K_b) of phenyl benzoates in micellar media.* Solutions of phenyl
7 benzoates were prepared in deionized water (MilliQ) and their concentration varied between 5.5×10^{-5} M
8 and 1.0×10^{-4} M. An aliquot (2 mL) of the phenyl benzoate solution was placed in fluorescence
9 stoppered quartz cuvette provided with a stirring bar and the UV-visible spectrum was recorded. The
10 initial absorbance value at the maximum absorption wavelength (A_0) was read. Subsequently, aliquots
11 of concentrated surfactant solution (10 μ L) were added. The UV-visible spectra were registered,
12 recording for each solution the A value at the maximum absorption wavelength. After each addition of
13 surfactant solution was stirred for 20 minutes before measuring the absorbance. With the values of A_0
14 and A in hands, the values of $(A_0/(A - A_0))$ versus the reciprocal of the concentration of the micellar
15 surfactant were plotted and the data were fitted with a linear regression program. The K_b values were
16 obtained calculating the ratio of the slope and the origin.

17
18
19
20
21
22
23
24
25
26
27
28
29
30
31
32 *Laser Flash Photolysis.* The laser pulse photolysis apparatus consisted of a Flash lamp-pumped Q-
33 switched SpitLight-100 Nd:YAG laser from InnoLas, used at the fourth harmonic of its fundamental
34 wavelength. The LP920-K monitor system (supplied by Edinburgh Instruments), arranged in a cross-
35 beam configuration, consisted of a high-intensity 450 W ozone free Xe arc lamp (operating in pulsed
36 wave), a Czerny-Turner with Triple Grating Turret monochromator, and a five-stage dynode
37 photomultiplier. The signals were captured by means of a Tektronix TDS 3012C digital phosphor
38 oscilloscope, and the data was processed with the L900 software supplied by Edinburgh Instruments.
39 The solutions to be analysed were placed in a fluorescence cuvette (d = 10 mm).

40
41
42
43
44
45
46
47
48
49
50
51
52
53 *Synthesis of phenyl benzoates 1 – 8.* To a solution of the substituted phenols (0.010 mol) in pyridine
54 (10 mL) cooled in an ice-bath, benzoyl chloride (0.012 mol) were added dropwise in 10 minutes under
55 stirring. Subsequently, the reaction mixture was kept under stirring for 60 minutes. After total
56
57
58
59
60

1
2 consumption of the starting material was confirmed by TLC, the reaction mixture was extracted with
3
4 dichloromethane (10 mL) and washed with a solution of diluted HCl (10 mL). The organic phase was
5
6 then washed with water, dried on Na₂SO₄, filtrated and evaporated under pressure. The phenyl
7
8 benzoates were purified from the solid residue by recrystallization using ethanol – water mixtures
9
10 giving the corresponding phenyl benzoates in excellent yields (> 90 %). The aryl benzoates **1** – **8** were
11
12 characterized comparing the physical constant (m.p.) and spectroscopic data (¹H-NMR and ¹³C-NMR)
13
14 with the ones reported in the literature.
15
16

17
18 *Photoirradiations of phenyl benzoates in homogeneous media.* A stock solution of a given benzoates (**1**
19
20 – **8**, 0.106 mmol in 200 mL cyclohexane) was placed in a stoppered Erlenmeyer quartz flask and
21
22 degassed with argon for 30 min. The flask was placed in a home made optical bench provided with the
23
24 possibility to use four or eighth lamps. The solution was stirred during the entire irradiation. Irradiations
25
26 with $\lambda_{\text{exc}} = 254$ nm were carried with four germicide lamps (Philips, each of 20 Watts, purchased in
27
28 Argentina). The reaction progress was monitored by TLC [eluent: hexane–ethyl acetate (8 : 2 v/v);
29
30 spots were visualized with UV light (254 and 366 nm)] and by GC analysis (Ultra 2 capillary column.
31
32 When the conversion of the starting material was higher than 90%, the photolyzed solution was
33
34 carefully evaporated to dryness under reduced pressure. The yellowish solid residue obtained was
35
36 purified by silica gel column chromatography (eluent: hexane 100% followed by hexane–ethyl acetate
37
38 mixtures). From the eluted fractions, the photoproducts were isolated and characterized by means of
39
40 physical and spectroscopic methods.
41
42
43
44
45

46
47 *Photoirradiations of phenyl benzoates in micellar media.* Stock solutions of surfactants in deionized
48
49 water (SDS 0.10 M and Brij-P35 0.05 M) were freshly prepared before each experiment. The aryl
50
51 benzoate (5 mg) was placed in a stoppered quartz cell provided with a stirring bar (3 ml) and the
52
53 surfactant stock solution (2 mL) was added. Then, the solution was vigorously stirred for one hour and
54
55 degassed with argon for 20 min. The quartz cell was placed in a homemade optical bench provided
56
57
58
59
60

with two germicide lamps (each of 20 W). The progress of the photoreaction was monitored by two different methods: (i) UV-visible spectroscopy and GC analysis (Ultra 2 capillary column). The conversion of the benzoates was kept below 20% to avoid secondary reactions and the formation of by-products. Previously to the injection into the GC apparatus, the micellar solutions were treated as follow. The photolyzed solutions were diluted with 2 mL of an aqueous solution of NaCl and then extracted with ethyl acetate (3x2 mL) while the system was carefully shaken to avoid the formation of emulsions. The organic layer was separated, dried over Na₂SO₄ and evaporated to dryness under vacuum. The yellowish solid residue was diluted in dichloromethane (2.00 mL) and this solution was injected into the GC for chromatographic analysis. The products were characterized by comparison of physical constant (m.p.) and spectroscopic data (¹H-NMR and ¹³C-NMR) with the ones reported in the literature.

p-Methoxyphenyl benzoate (**1**). White needles (2.24 g; 98 %). M. p.: 89-90°C (lit. 87-88°C²²). ¹H NMR (300 MHz, CDCl₃): δ 8.23 (d, *J* = 8.6 Hz, *J* = 1.4 Hz, 2H), 7.66 (dd, *J* = 8.6 Hz, *J* = 1.3 Hz, 2H), 7.53 (t, *J* = 7.8 Hz, *J* = 1.1 Hz, 1H), 7.17 (d, *J* = 9.4 Hz, 2H), 6.97 (d, *J* = 9.4 Hz, 2H), 3.85 (s, 3H). ¹³C{¹H} NMR (75 MHz, CDCl₃): δ 165.4, 157.2, 144.3, 133.4, 130.0, 129.6, 128.4, 122.3, 114.4, 55.5.

p-Phenoxyphenyl benzoate (**2**). White plates (2.84 g; 98 %). M. p.: 100-101°C²³. ¹H NMR (300 MHz, CDCl₃): δ 8.24 (d, *J* = 7.1, 1.0 Hz, 2H), 7.67 (t, *J* = 7.7 Hz, 1H), 7.55 (t, *J* = 7.9 Hz, 2H), 7.39 (t, *J* = 8.4 Hz, 2H), 7.21 (d, *J* = 8.9 Hz, 2H), 7.18 – 7.04 (m, 5 H). ¹³C{¹H} NMR (75 MHz, CDCl₃): δ 165.2, 157.1, 146.2, 133.5, 130.1, 129.7, 129.4, 128.5, 123.5, 122.7, 119.6, 118.7.

p-Methylphenyl benzoate (**3**). White needles (2.02 g; 95 %). M. p.: 71°C (lit. 72°C²⁴). ¹H NMR (300 MHz, CDCl₃): δ 8.24 (d, *J* = 8.2 Hz, *J* = 1.4 Hz, 2H), 7.65 (dd, *J* = 7.4 Hz, *J* = 1.2 Hz, 2H), 7.54 (t, *J* = 7.8 Hz, *J* = 1.2 Hz, 1H), 7.25 (d, *J* = 8.3 Hz, 2H), 7.13 (d, *J* = 8.5 Hz, 2H), 2.41 (s, 3H). ¹³C{¹H} NMR (75 MHz, CDCl₃): δ 165.3, 148.6, 135.4, 133.4, 130.1, 129.6, 129.9, 128.4, 121.3, 20.8.

p-*t*-Butylphenyl benzoate (**4**). White plates (2.44 g; 96 %). M. p.: 83-84°C (lit. 82-83°C²⁵). ¹H NMR (300 MHz, CDCl₃): δ 8.23 (dd, *J* = 7.9, 1.6 Hz, 2H), 7.66 (t, *J* = 7.4 Hz, 2H), 7.55 (t, *J* = 8.7 Hz, 1H),

1
2 7.47 (d, $J = 8.7$ Hz, 2H), 7.17 (d, $J = 8.7$ Hz, 2H), 1.35 (s, 9H). $^{13}\text{C}\{^1\text{H}\}$ NMR (75 MHz, CDCl_3): δ
3 165.2, 148.6, 148.5, 133.4, 130.0, 129.6, 128.4, 126.3, 120.9, 34.4, 31.6.

4
5
6 *Phenyl benzoate (5)*. White solid (1.94 g; 98 %). M. p.: 69-70°C (lit. 67-69°C^{6a}). ^1H NMR (300 MHz,
7 CDCl_3): δ 8.25 (d, $J = 7.4$ Hz, 2H), 7.67 (t, $J = 7.6$ Hz, 1H), 7.55 (t, $J = 8.1$ Hz, 2H), 7.45 (t, $J = 8.3$,
8 7.8 Hz, 2H), 7.32 (t, $J = 8.1$, 7.2 Hz, 1H), 7.24 (d, $J = 7.2$ Hz, 2H). $^{13}\text{C}\{^1\text{H}\}$ NMR (75 MHz, CDCl_3): δ
9 165.1, 150.9, 133.5, 130.1, 129.5, 129.4, 128.5, 125.8, 121.6.

10
11
12
13
14
15 *p*-Phenylphenyl benzoate (6). White needles (2.52 g; 92 %). M. p.: 150-151°C.²³ ^1H NMR (300 MHz,
16 CDCl_3): δ 8.20 (d, $J = 8.2$, 1.2 Hz, 2H), 7.72 – 7.61 (m, 5H), 7.57 (t, $J = 7.9$ Hz, 2H), 7.49 (t, $J = 7.8$
17 Hz, 2H), 7.41 (d, $J = 7.2$ Hz, 1H), 7.33 (d, $J = 8.6$ Hz, 2H). $^{13}\text{C}\{^1\text{H}\}$ NMR (75 MHz, CDCl_3): δ 165.1,
18 150.3, 140.3, 138.9, 133.5, 130.1, 129.4, 128.7, 128.5, 128.1, 127.3, 127.0, 121.9.

19
20
21
22
23
24 *p*-Cyanophenyl benzoate (7). White solid (2.01 g; 90 %). M. p.: 94-95°C (lit. 91-92°C²⁶). ^1H NMR (300
25 MHz, CDCl_3) δ : 8.22 (d, $J = 8.4$ Hz, 2H), 7.74 (d, $J = 7.64$ Hz 2H), 7.70 (t, $J = 7.0$, 7.64Hz, 2H) 7.56 (t,
26 $J = 7.6$ Hz, 2H), 7.4 (d, $J = 8.4$ Hz, 2H). $^{13}\text{C}\{^1\text{H}\}$ NMR (75 MHz, CDCl_3) δ : 164.2, 154.1, 134.0, 133.6,
27 130.1, 128.6, 128.5, 122.8, 118.2, 109.7.

28
29
30
31
32
33 *p*-Nitrophenyl benzoate (8). Pale yellow needles (2.21 g; 91 %). M. p.: 144-145°C (lit. 142 – 144°C²⁷).
34 ^1H NMR (300 MHz, CDCl_3) δ : 8.34 (d, $J = 9.1$ Hz, 2H), 8.23 (dd, $J = 7.6$, 1.3 Hz, 2H), 7.71 (t, $J = 7.5$
35 Hz, 1H), 7.57 (t, $J = 7.5$ Hz, 2H), 7.45 (d, $J = 9.1$ Hz, 2H). $^{13}\text{C}\{^1\text{H}\}$ NMR (75 MHz, CDCl_3) δ : 164.1,
36 155.6, 145.3, 134.2, 130.2, 128.7, 128.4, 125.2, 122.5.

37
38
39
40
41
42
43 *2*-Hydroxy-5-methoxybenzophenone (1a). Pale yellow needles (188 mg; 94 %). M. p.: 83 – 84°C (lit.
44 84°C²⁸). ^1H NMR (300 MHz, CDCl_3) δ : 11.58 (s, 3H); 7.69 (dd, $J = 8.5$, 1.6 Hz, 2H), 7.60 (t, $J = 7.5$
45 Hz, 1H), 7.51 (t, $J = 7.8$ Hz, 2H), 7.14 (d, $J = 9.0$, 2.9 Hz, 1H), 7.06 (d, $J = 3.1$ Hz, 1H), 7.02 (d, $J = 9.0$
46 Hz, 1H), 3.70 (s, 3H). $^{13}\text{C}\{^1\text{H}\}$ NMR (75 MHz, CDCl_3) δ : 201.1, 157.7, 151.6, 138.0, 132.1, 130.3,
47 129.2, 128.5, 124.3, 119.4, 116.5, 56.1.

48
49
50
51
52
53
54
55 *2*-Hydroxy-5-phenoxybenzophenone (2a). Yellow needles (193 mg; 76 %). M. p.: 47 – 48 °C. ^1H NMR
56 (300 MHz, CDCl_3) δ : 11.85 (s, 1H), 7.70 (d, $J = 8.1$ Hz, 2H), 7.59 (t, $J = 7.4$, 1H), 7.50 (t, $J = 7.6$ Hz,
57
58
59
60

2H), 7.34 – 7.26 (m, 4 H), 7.12 (d, $J = 8.7$ Hz, 1H), 7.07 (t, $J = 7.4$ Hz, 1H), 6.94 (d, $J = 8.7$ Hz, 2H).
 $^{13}\text{C}\{^1\text{H}\}$ NMR (75 MHz, CDCl_3) δ : 200.9, 159.6, 158.6, 147.7, 137.5, 132.2, 129.8, 129.2, 128.9,
128.5, 123.8, 122.8, 119.7, 119.2, 117.3. Anal. Calcd for $\text{C}_{19}\text{H}_{14}\text{O}_3$: C, 78.61; H, 4.86. Found: C, 78.57;
H, 4.90.

2-Hydroxy-5-methylbenzophenone (3a). Pale yellow needles (130 mg; 70 %). M. p.: 83-84°C (lit. 84°C²⁹). ^1H NMR (300 MHz, CDCl_3) δ : 11.84 (s, 1H), 7.67 (dd, $J = 8.4, 1.2$ Hz, 2H), 7.60 (t, $J = 7.4, 1\text{H}$), 7.52 (t, $J = 7.8$ Hz, 2H), 7.36 (d, $J = 2.8$ Hz, 1 H), 7.32 (dd, $J = 8.5, 2.3$ Hz, 1H), 6.98 (d, $J = 8.54$ Hz, 1H), 2.28 (s, 3H). $^{13}\text{C}\{^1\text{H}\}$ NMR (75 MHz, CDCl_3) δ : 201.7, 161.3, 138.2, 137.5, 133.3, 131.9, 129.2, 128.5, 127.9, 118.9, 118.3, 20.6.

*2-Hydroxy-5-*t*-butylbenzophenone (4a)*. White solid (189 mg; 85 %). M. p.: 67-68°C (lit. 67 – 68°C²⁵). ^1H NMR (300 MHz, CDCl_3) δ : 11.87 (s, 1 H), 7.72 (dd, $J = 1.6, 8.1$ Hz, 2H), 7.63 (t, $J = 1.3, 7.4, 2\text{H}$), 7.60 (t, $J = 2.5, 8.5$ Hz, 1H), 7.55 (t, $J = 1.6, 7.2$ Hz, 2 H), 7.05 (d, $J = 8.3$ Hz, 1H), 1.28 (s, 9H). $^{13}\text{C}\{^1\text{H}\}$ NMR (75 MHz, CDCl_3) δ : 201.6, 161.0, 141.3, 138.1, 133.9, 131.9, 129.8, 129.3, 128.3, 118.4, 117.9, 34.1, 31.3.

2-Hydroxybenzophenone (5a). Yellow needles (156 mg; 90 %). M. p.: 37-38°C (lit. 37 – 38°C^{6a}). ^1H NMR (300 MHz, CDCl_3) δ : 12.05 (s, 1H), 7.68 (dd, $J = 1.4, 8.4$ Hz, 2H), 7.61 – 7.57 (m, 2H), 7.53 – 7.48 (m, 3H), 7.08 (dd, $J = 1.1, 8.5$ Hz, 1 H), 6.88 (dd, $J = 1.1, 7.2$ Hz, 1H). $^{13}\text{C}\{^1\text{H}\}$ NMR (75 MHz, CDCl_3) δ : 201.7, 163.3, 138.0, 136.4, 133.7, 132.0, 129.3, 129.2, 128.5, 119.2, 118.8, 118.5, 118.3.

4-Hydroxybenzophenone. Yellow plates (14 mg; 8 %). M. p.: 133-134°C (lit. 133 – 134°C^{6a,30}). ^1H NMR (300 MHz, CDCl_3) δ : 7.77 (d, $J = 8.8$ Hz, 2H), 7.75 (d, $J = 8.4, 2\text{H}$), 7.57 (t, $J = 7.4, 1.3$ Hz, 1H), 7.47 (t, $J = 7.5$ Hz, 2 H), 6.95 (d, $J = 8.7$ Hz, 2H). $^{13}\text{C}\{^1\text{H}\}$ NMR (75 MHz, CDCl_3) δ : 197.2, 161.1, 138.1, 133.3, 132.4, 130.0, 129.5, 128.4, 115.6.

2-Hydroxy-5-phenyl benzophenone (6a). White needles (209 mg; 87 %). M. p.: 91-92°C (lit. 91 – 92°C³¹). ^1H NMR (300 MHz, CDCl_3) δ : 12.06 (s, 1 H), 7.80 (dd, $J = 2.4, 8.6$ Hz, 1H), 7.77 (dd, $J = 1.5, 8.5, 2\text{H}$), 7.70 – 7.62 (m, 2H), 7.56 (t, $J = 7.7, 1.7$ Hz, 2H), 7.49 (dd, $J = 8.5, 1.4$ Hz, 2 H), 7.44 (t, $J =$

1
2 7.5, 1.5 Hz, 2H), 7.35 (t, $J = 7.2$ Hz, 1H), 7.21 (d, $J = 8.6$ Hz, 1H). $^{13}\text{C}\{^1\text{H}\}$ NMR (75 MHz, CDCl_3) δ :
3
4 201.7, 162.6, 139.8, 137.9, 135.1, 133.7, 132.1, 132.0, 131.8, 129.3, 128.9, 128.8, 128.5, 119.3, 118.9.

5
6 *2-Hydroxy-5-cyano benzophenone (7a)*. Pale yellow needles (156 mg; 80 %). M. p.: 120-121°C (lit.
7
8 120 – 121°C³²). ^1H NMR (300 MHz, CDCl_3) δ : 12.48 (s, 1H), 7.96 (d, $J = 2.1$, 1H), 7.74 (dd, $J = 8.7$,
9
10 2.1 Hz, 1H), 7.70 – 7.65 (m, 3H), 7.60 – 7.55 (m, 2H), 7.16 (d, $J = 8.7$ Hz, 1H). $^{13}\text{C}\{^1\text{H}\}$ NMR (75
11
12 MHz, CDCl_3) δ : 200.6, 166.4, 138.7, 138.4, 136.6, 133.1, 129.3, 129.0, 120.2, 119.4, 118.3, 102.6.

13
14
15 *2-Hydroxy-5-nitro benzophenone (8a)*. Intense yellow plates (94 mg; 44 %). M. p.: 123-124°C (lit. 123
16
17 – 124°C³³). ^1H NMR (300 MHz, CDCl_3) δ : 12.67 (s, 1H), 8.60 (d, $J = 2.7$ Hz, 1H), 8.40 (dd, $J = 9.2$,
18
19 2.7 Hz, 1H), 7.72 (d, $J = 8.4$, 1.3 Hz, 2H), 7.69 (t, $J = 7.5$, 1.3 Hz, 1H), 7.59 (t, $J = 7.8$, 1.8 Hz, 2H),
20
21 7.19 (d, $J = 9.2$ Hz, 1H). $^{13}\text{C}\{^1\text{H}\}$ NMR (75 MHz, CDCl_3) δ : 200.7, 168.1, 139.6, 136.5, 133.3, 131.1,
22
23 129.8, 129.4, 129.2, 119.7, 118.1.
24
25
26
27
28

29 Acknowledgement.

30
31 The authors thank Universidad de Buenos Aires (X 0055BA), CONICET (PIP0072CO and PIP0505)
32
33 and ANPCyT (PICT 2012-0888) for financial support. S.M.B. is a research member of CONICET.
34
35
36
37

38 Supporting Information.

39
40 UV-visible absorption spectra under steady-state and time-resolved spectroscopy. Relative absorption
41
42 profiles. Determination of the constants of binding K_b . 2D NOESY NMR spectra in micellar media.
43
44 Determination of the rate constants k_E and k_R in homogeneous and heterogeneous media. Copy of the
45
46 ^1H and ^{13}C spectra of aryl benzoates and of 2-hydroxy-5-substituted benzophenones. This material is
47
48 available free of charge via the Internet at <http://pubs.acs.org>.
49
50
51
52
53

54 References.

- 1
2 1. (a) Miranda, M. A.; Galindo, F. in *Photochemistry of Organic Molecules in isotropic and*
3 *Anisotropic Media*, eds. Ramamurthy, V. and Schanze, K. S., Marcel Dekker, New York, 2003,
4 Chapter 2; (b) Natarajan, A.; Kaanumale, L. S.; Ramamurthy, V. in *CRC Handbook of Organic*
5 *Photochemistry and Photobiology*, eds. Horspool, W. and Lenci, F., CRC Press, Boca Raton, FL, 2004,
6 Vol. 3, p. 107; (c) Fendler, J. H.; Fendler, E. J. in *Catalysis in Micellar and Macromolecular System*,
7 Academic Press, London, 1975; (d) *Mixed Surfactant System*, eds. Holland, P. M. and Rubingh, D. N.,
8 American Chemical Society, Washington, DC, 1994; (e) Turro, N. J., From Boiling Stones to Smart
9 Crystals: Supramolecular and Magnetic Isotope Control of Radical–Radical Reactions in Zeolites, *Acc.*
10 *Chem. Res.*, **2000**, *33*, 637-646.
11
12 2. a) Turro, N. J.; Mattay, J., Photochemistry of some deoxybenzoines in micellar solution. Cage
13 effects, isotop effects, and magnetic field effects, *J. Am. Chem. Soc.*, **1981**, *103*, 4200-4204; b) Turro,
14 N. J.; Sidney Cox, G.; Paczkowski, M. A. *Photochemistry in Micelles in Topics in Current Chemistry*,
15 Photochemistry and Organic Synthesis, ed. F.L. Boschke, *Springer-Verlag, New York*, 1985, **129**, 57.
16
17 3. a) Turro, N. J.; Kraeutler, B., Magnetic field and magnetic isotope effects in organic photochemical
18 reactions. A novel probe of reaction mechanisms and a method for enrichment of magnetic isotopes,
19 *Acc. Chem. Res.*, 1980, **13**, 369-377; b) Turro, N. J.; Buchachenko, A. L.; Tarasov, V. F., How spin
20 stereochemistry severely complicates the formation of a carbon-carbon bond between two reactive
21 radicals in a supercage, *Acc. Chem. Res.*, 1995, **28**, 69-80; c) Lalyanasundaran, K. in *Photochemistry in*
22 *Microheterogeneous Systems*, Academic Press, Inc., Orlando, FL, 1987.
23
24 4. Anderson, J. C.; Reese, C. B., Photo-induced Fries rearrangement, *Proc. Chem. Soc. London*, **1960**,
25 217.
26
27 5. (a) Bellus, D., Photo-Fries rearrangement and related photochemical [1,j]-shifts (j = 3, 5, 7) of
28 carbonyl and sulfonylgroups, *Adv. Photochem.*, **1971**, *8*, 109-159; (b) Miranda, M. A. in *CRC*
29 *Handbook of Organic Photochemistry and Photobiology*, eds. W. Horspool, P. S. Song, CRC Press,
30 Boca Raton, FL, 1995, p. 570. (c) Bellus, B.; Hdrlovich, P., Photochemical rearrangement of aryl, vinyl
31
32
33
34
35
36
37
38
39
40
41
42
43
44
45
46
47
48
49
50
51
52
53
54
55
56
57
58
59
60

1 and substituted vinyl esters and amides of carboxylic acids, *Chem. Rev.*, **1967**, *67*, 599 – 609. (d)
2
3
4 Photo-Fries Rearrangement in *Comprehensive Organic Name Reactions and Reagents*. **2010**, 497, p
5
6 2200–2205. (e) Kobsa, H., Rearrangement of aromatic esters by ultraviolet radiation, *J. Org. Chem.*,
7
8 **1962**, *27*, 2293-2298. (f) Sandner, M. R.; Trecker, D. J., Mechanism of the photo-Fries reaction, *J. Am.*
9
10 *Chem. Soc.*, **1967**, *89*, 5725-5726. (g) Jimenez, M. C.; Miranda, M. A.; Scaiano, J. C.; Tormos, R.,
11
12 Two-photon processes in the photo-Claisen and photo-Fries rearrangements. Direct observation of
13
14 diene ketenes generated by photolysis by transient cyclohexa-2,4-dienones, *Chem. Commun.*, **1997**,
15
16 1487-1488. (h) Lochbrunner, S.; Zissler, M.; Piel, J.; Riedle, E., Real time observation of the photo-
17
18 Fries rearrangement, *J. Chem. Phys.*, **2004**, *120*, 11634- 11639. (i) Norell, J. R., Organic reactions in
19
20 liquid hydrogen fluoride. IV Fries rearrangement of aryl benzoates, *J. Org. Chem.* **1973**, *38*, 1924-
21
22 1928. (j) Park, K. K.; Lee, J. J.; Ryu, J., Photo-Fries rearrangement of N-aryl sulfonamides to
23
24 aminoaryl sulfone derivatives, *Tetrahedron* **2003**, *59*, 7651 – 7659.

25
26
27
28
29 6. (a) Meyer, J. W.; Hammond, G. S., Mechanism of photochemical reactions in solution. LXX.
30
31 Photolysis of aryl esters, *J. Am. Chem. Soc.*, **1972**, *94*, 2219-2228. (b) Kalmus, C. E.; Hercules, D. S.,
32
33 Mechanistic studies of the photo-Fries rearrangement of phenyl acetate, *J. Am. Chem. Soc.*, **1974**, *96*,
34
35 449-460. (c) Gristan, N. P.; Tsentalovich, Y. P.; Yurkovskay, A. V.; Sagdeev, R. Z., Laser flash
36
37 photolysis and CIDNP studies of 1-naphthyl acetate phto-Fries rearrangement, *J. Phys. Chem.*, **1996**,
38
39 *100*, 4448-4458; (d) Bonesi, S. M.; Crevatin, L. K.; Erra Balsells, R., Photochemistry of 2-
40
41 acyloxycarbazoles. A potential tool in the synthesis of carbazole alkaloids, *Photochem. Photobiol. Sci.*,
42
43 **2004**, *3*, 381 – 388; (e) Crevatin, L. C.; Bonesi, S. M.; Erra Balsells, R., Photo-Fries rearrangement of
44
45 carbazol-2-yl sulfonates: efficient tool for the introduction of sulfonyl groups into polycyclic aromatic
46
47 compounds, *Helv. Chim. Acta*, **2006**, *89*, 1147 – 1157.

48
49
50
51
52 7. (a) Sandner, M. R.; Hedaya, E.; Tecker, D. J., Mechanistic studies of the photo-Fries reaction, *J. Am.*
53
54 *Chem. Soc.*, **1968**, *90*, 7249 – 7254. (b) Coppinger, G. M.; Bell, E. R., Photo-Fries rearrangement of
55
56 aromatic esters. Role of steric and electronic factors, *J. Phys. Chem.*, **1966**, *70*, 3479 – 3489. (c)
57
58
59

- 1
2 Sharma, P. K.; Khanna, N. R., Photo-Fries rearrangement: rearrangement of benzoyloxy compounds,
3
4 *Monast. Fur Chemie*, **1985**, *116*, 353 – 356. (d) Finnegan, R. A.; Mattice, J. J., Photochemical studies.
5
6 II. The photo rearrangement of aryl esters, *Tetrahedron*, **1965**, *21*, 1015 – 1016. (e) Adam, W, Sanabia,
7
8 J. A.; Fischer, H., CIDNP evidence for radical pair mechanism in photo-Fries rearrangement, *J. Org.*
9
10 *Chem.*, **1973**, *38*, 2571 – 2572. (f) Adam, W., The multiplicity of the photo-Fries rearrangement, *Chem.*
11
12 *Commun.* **1974**, 289 – 290. (g) Stumpe, J.; Selbmann, Ch.; Kreyzig, D., Photoreactions in liquid crystal
13
14
15 2. Photo-Fries rearrangement of aromatic esters in liquid crystalline matrices, *J. Photochem. Photobiol.*
16
17 *A:Chem*, **1991**, *58*, 15 – 30.
18
19
20 8. (a) Singh, A. K.; Raghuraman, T. S., Photorearrangement of phenyl cinnamates under micellar
21
22 environment, *Tetrahedron Lett.*, **1985**, *26*, 4125-4128. (b) Singh, A. K.; Raghuraman, T. S.,
23
24 Photorearrangement of aryl esters in micellar medium, *Synth. Commun.*, **1986**, *16*, 485-490. (c) Xie, R.
25
26 Q.; Liu, Y. C.; Lei, X. G., The photo-Fries rearrangement of α -naphthyl acetate in cyclodextrin and
27
28 micelle, *Res. Chem. Intermed.*, **1992**, *18*, 61-69. (d) Nasetta, M.; De Rossi, R. H.; Cosa, J. J., Influence
29
30 of cyclodextrine on the photo-Fries rearrangement of acetanilide, *Can. J. Chem.*, **1988**, *66*, 2794-2798.
31
32 (e) Pitchumani, K.; Warriar, M.; Ramamurthy, V., Remarkable product selectivity during Photo-Fries
33
34 and photo-claisen rearrangements within zeolites, *J. Am. Chem. Soc.*, **1996**, *118*, 9428 – 9429.
35
36
37 9. Iguchi, D.; Erra-Balsells, R.; Bonesi, S. M., Photo-Fries rearrangement of aryl acetamides:
38
39 regioselectivity induced by the aqueous micellar green environment, *Photochem. Photobiol. Sci.*, **2016**,
40
41 *15*, 105 – 116.
42
43
44 10. (a) Morohoshi, K.; Yamamoto, H.; Kamata, R.; Shiraishi, F; Koda, T.; Morita, M., estrogenic
45
46 activity of 37 componets of commercial sunscreen lotions evaluated by in vitro assays, *Toxicology in*
47
48 *vitro*, **2005**, *19*, 457 – 469. (b) Venu, T. D.; Shashikauth, S.; Khanun, S. A.; Naveen, S.; Firdouse, A.;
49
50 Sridhar, M. A.; Shashidhara Prasad, J., Synthesis and crystallographic analysis of benzophenone
51
52 derivatives. The potential anti-inflammatory agents, *Bioorg. Med. Chem.*, **2007**, *15*, 3505 – 3514. (c)
53
54 Coronado, M.; De Haro, H.; Deng, X.; Rempel, M. A.; Lavado, R.; Schlenck, D., Estrogenic activity
55
56
57
58
59
60

1
2 and reproductive effects of the UV-filter oxybenzone (2-hydroxy-4-methoxyphenyl-methanone) in fish,
3
4 *Aquatic Tox.*, **2008**, *90*, 182 – 187. (d) Maciel Rezende, C. M.; de Almeida, L.; Costa, E. D.; Robeiro
5
6 Pires, F.; Ferreira Alves, K.; Viegas Junior, C.; Ferreira Dias, D.; Dominguetto, A. C.; Marques, M. J.;
7
8 Dos Santos, M. H., Synthesis and biological evaluation against *Leishmania amazonensis* of a series of
9
10 alkyl-substituted benzophenones, *Bioorg. Med. Chem.*, **2013**, *21*, 3114 – 3119.

11
12
13 11. (a) Tachikawa, Y.; Cui, L.; Matsusaki, Y.; Tada, N.; Miura, T.; Itoh, A., Aerobic photooxidative
14
15 cleavage of 1,3-diketones to carboxylic acids using 2-chloroanthraquinone, *Tetrahedron Letters* **2013**,
16
17 *54*, 6218–6221. (b) McNesby, J. R.; Heller, C. A., Oxidation of liquid aldehydes by molecular oxygen,
18
19 *Chem. Rev.*, **1954**, *54*, 325–346.

20
21
22 12. Goldstein, S.; Rabani, J., The ferrioxalate and iodide-iodate actinometers in the UV region, *J.*
23
24 *Photochem. Photobiol., Chem.: A* **2008**, *193*, 50-55.

25
26
27 13. Dichiarante, V.; Dondi, D.; Protti, S.; Fagnoni, M.; Albini, A., A meta effect in organic
28
29 photochemistry? The case of S_N1 reactions in methoxyphenyl derivatives, *J. Am. Chem. Soc.*, **2007**,
30
31 *129*, 5605 - 5611; correction: **2007**, *129*, 11662.

32
33
34 14. (a) Turro, N. J. in *Modern Molecular Photochemistry*, The Benjamin Cummings Publishing
35
36 Company, Menlo Park, California, 1978. (b) Turro, N. J.; Ramamurthy, V.; Scaiano, J. C. in *Modern*
37
38 *Molecular Photochemistry of Organic Molecules*, University Science Books, Sausalito, California,
39
40 2010.

41
42
43 15. (a) Bonesi, S. M.; Mesaros, M.; Cabrerizo, F. M.; Ponce, M. A.; Bilmes, G.; Erra Balsells, R., The
44
45 photophysics of nitrocarbazoles used as UV-MALDI matrices: comparative spectroscopic and
46
47 optoacoustic studies of mononitro- and dinitrocarbazoles, *Chem. Phys. Lett.*, **2007**, *446*, 49 – 55. (b)
48
49 Cors, A.; Bonesi, S. M.; Erra Balsells, R., Photoreduction of nitro arenes by formic acid in acetonitrile
50
51

52
53 **DOI: 10.1021/acs.joc.5b01177**

54
55 16. (a) Sepulveda, L.; Lissi, E. Quina, F. H., Interactions of Neutral Molecules with Ionic Micelles, *Adv.*
56
57 *Colloid Interface Sci.*, **1986**, *25*, 1–57; (b) Quina, F. H.; Alonso, E. O., Incorporation of Nonionic Solutes
58
59

- 1
2 into Aqueous Micelles: A Linear Solvation Free Energy Relationship Analysis, *J. Phys. Chem.*, **1995**, *99*,
3
4 11708–11714; (c) Abraham, H.; Chadha, H. S.; Dixon, J. P.; Rafols, C.; Treiner, C., Hydrogen bonding
5
6 Part 40. Factors that influence the distribution of solutes between water and sodium dodecylsulfate
7
8 micelles, *J. Chem. Soc., Perkin Trans. 2*, **1995**, 887–894; (d) Abraham, H.; Chadha, H. S.; Dixon, J. P.
9
10 ; Rafols, C.; Treiner, C., Hydrogen bonding. Part 41.1 Factors that influence the distribution of solutes
11
12 between water and hexadecylpyridinium chloride micelles, *J. Chem. Soc., Perkin Trans. 2*, **1997**, 19–
13
14 24.
15
16
17
18 17. Brinchi, L.; di Profio, P.; Micheli, F.; Germani, R.; Savelli, G.; Bunton, C. A., Structure of Micellar
19
20 head-Groups and the Hydrolysis of Phenyl Chlorofomate. The Role of Perchlorate Ion, *Eur. J. Org.*
21
22 *Chem.*, **2001**, 1115 – 1120.
23
24
25 18. Campos Rey, P.; Cabaleiro Lago, C.; Hervés, P., Solvolysis of Substituted benzoyl Chlorides in
26
27 Nonionic and Mixed Micellar Solutions, *J. Phys. Chem. B*, **2010**, *114*, 14004–14011.
28
29
30 19. (a) Sabatino, P.; Szczygiel, A.; Sinnaeve, D.; Hakimhashemi, M.; Saveyn, H.; Martins, J. C.; van
31
32 der Meeren, P., NMR study of the influence of pH on phenol sorption in cationic CTAB micellar
33
34 solutions, *Colloids and Surfaces A: Physicochem. Eng. Aspects* **2010**, *370*, 42 – 48. (b) Voets, I. K.; de
35
36 Keizer, A.; de Waard, P.; Frederik, P. M.; Bomans, P. H. H.; Schmalz, H.; Walther, A.; King, S. M.;
37
38 Leermakers, F. A. M.; Cohen Stuart, M. A., Doubled-faced micelles from water-soluble polymers,
39
40 *Angew. Chem. Int. Ed.* **2006**, *45*, 6673 – 6676. (c) Yuan, H. Z.; Zhao, S.; Cheng, G. Z.; Zhang, L.;
41
42 Miao, X. J.; Mao, S. Z.; Yu, J. Y.; Shen, L. F.; Du, Y. R., Mixed micelles of Triton X-100 and Cetyl
43
44 triammonium bromide in aqueous solution studied by 1h NMR, *J. Phys. Chem. B* **2001**, *105*, 4611-
45
46 4615.
47
48
49
50 20. (a) Das, P. K.; Encinas, M. V.; Steenken, S.; Scaiano, J. C., Reaction of t-butoxy radicals with
51
52 phenols. Comparison with the reactions of carbonyl triplets, *J. Am. Chem. Soc.* **1981**, *103*, 4162-4166.
53
54 (b) Land, E. J.; Porter, G.; Strachan, E., Primary photochemical processes in aromatic molecules. Part
55
56 6. The absorption spectra and acidity constants of phenoxyl radicals, *Trans. Faraday Soc.* **1961**, *57*,

- 1
2 1885-1893. (c) Land, E. J.; Porter, G., Primary photochemical processes in aromatic molecules. Part 7.
3
4 Spectra and kinetics of some phenoxy derivatives, *Trans. Faraday Soc.* **1963**, *59*, 2016-2026. (d)
5
6 Land, E. J.; Ebert, M., Pulse radiolysis studies of aqueous phenol. Water elimination from
7
8 dihydroxycyclohexadienyl radicals to form phenoxy, *Trans. Faraday Soc.* **1967**, *63*, 1181-1190. (e)
9
10 Gadosy, T. A.; Shukla, D.; Johnston, L. J., Generation, characterization, and deprotonation of phenol
11
12 radical cations, *J. Phys. Chem. A* **1999**, *103*, 8834-8839. (f) Alfassi, Z. B.; Schuler, R. H., Reaction of
13
14 azide radicals with aromatic compounds. Azide as a selective oxidant, *J. Phys. Chem.* **1985**, *89*, 3359-
15
16 3363. (g) Ganapathi, M. R.; Hermann, R.; Naumov, S.; Brede, O., free electron transfer from several
17
18 phenols to radical cations of non-polar solvents, *Phys. Chem. Chem. Phys.*, **2000**, *2*, 4947 – 4955.
19
20
21 21. Bonesi, S. M.; Crespi, S.; Merli, D.; Manet, I.; Albini, A., Direct irradiation of aryl sulfides:
22
23 hemolytic fragmentation and sensitized S-oxidation, *J. Org. Chem.* **2017**, *82*, 9054–9065.
24
25
26 22. Chen, C.-T.; Munot, Y. S., Direct atom-efficient esterification between carboxylic acids and
27
28 alcohols catalyzed by atmospheric, water-tolerant TiO(acac)₂, *J. Org. Chem.* **2005**, *70*, 8625 – 8627.
29
30
31 23. Seni, A. A., Kollar, L.; Mika, L. T.; Pongracz, P., Rhodium-catalysed aryloxyacylation of
32
33 iodo-aromatics by 4-substituted phenols with carbon monoxide or paraformaldehyde, *Molecular*
34
35 *Catalysis*, **2018**, *457*, 67 – 73.
36
37
38 24. Singh, A. K.; Sonar, S. M., Photorearrangement of aryl esters in micellar medium, *Synth. Commun.*
39
40 **1985**, *15*, 1113 – 1122.
41
42
43 25. Kobsa, H., Rearrangement of Aromatic esters by ultraviolet radiation, *J. Org. Chem.* **1962**, *27*,
44
45 2293 – 2298.
46
47
48 26. (a) Ariswa, M.; Igarashi, Y.; Kobayashi, H.; Yamada, T.; Bando, K.; Ichikawa, T.; Yamaguchi, M.,
49
50 Equilibrium shift in the rhodium-catalyzed acyl transfer reactions, *Tetrahedron* **2011**, *67*, 7846 – 7859.
51
52 (b) Neuvonen, H.; Neuvonen, K.; Pasanen, P., Evidence of Substituent-Induced Electronic Interplay.
53
54 Effect of the Remote Aromatic Ring Substituent of Phenyl Benzoates on the Sensitivity of the
55
56
57
58
59
60

1
2 Carbonyl Unit to Electronic Effects of Phenyl or Benzoyl Ring Substituents, *J. Org. Chem.* **2004**, *69*,
3
4 3794 - 3800.

5
6
7 27. Kim, S.; Lee, J. I.; Kim, Y. C., A simple and mild esterification method for carboxylic acids using
8
9 mixed carboxylic-carbonic anhydrides, *J. Org. Chem.* **1985**, *50*, 560 – 565.

10
11 28. Martin, R., Studies on the Friedel-Craft reaction. Preparation of isomeric 2-acyl- and 3-acyl-4-
12
13 methoxy phenols, *Monatshefte fur Chemie* **1981**, *112*, 1155 – 1163.

14
15
16 29. Sander, M. R.; Hedaya, E.; Trecker, D. J., Mechanistic studies of the photo-Fries rearrangement, *J.*
17
18 *Am. Chem. Soc.* **1968**, *90*, 7249.

19
20 30. Cheung, C. W.; Buchwald, S. L., Palladium-catalyzed hydroxylation of aryl and heteroarylhalides
21
22 enabled by the use of a Palladacycle precatalyst, *J. Org. Chem.* **2014**, *79*, 5351–5358.

23
24 31. (a) Gu, Y.; Wu, F.; Yang, J., Oxidative [3+3] annulation of atropaldehyde acetals with 1,3-
25
26 bisnucleophiles: an efficient method of constructing six-membered aromatic rings, including salicylates
27
28 and carbazoles, *Advances Synth. Catal.* **2018**, *360*, 2727 – 2741. (b) Xie, Y., Acylation of Csp²-H bond
29
30 with acyl sources derived from alkynes Rh-Cu bimetallic catalyzed C-C bond cleavage, *Chem.*
31
32 *Commun.* **2016**, *52*, 12372 – 12375.

33
34
35
36 32. Yaegashi, T.; Nunomura, S.; Okutome, T.; Nakayama, T.; Kurumi, M.; Sakurai, Y.; Aoyama, T.;
37
38 Fujii, S., Synthesis and structure-activity of protease inhibitors. III. Amidinophenols and their benzoyl
39
40 esters, *Chem. Pharm. Bull.* **1984**, *32*, 4466 – 4477.

41
42
43 33. Martin, R. *Substituted Hydroxybenzophenone (Class of Methanones) in Aromatic Hydroxyketones:*
44
45 *Preparation and Physical Properties*. Springer, Dordrecht, 2011.